

## **Distribution Agreement**

In presenting this thesis as a partial fulfillment of the requirements for a degree from Emory University, I hereby grant to Emory University and its agents the non-exclusive license to archive, make accessible, and display my thesis in whole or in part in all forms of media, now or hereafter now, including display on the World Wide Web. I understand that I may select some access restrictions as part of the online submission of this thesis. I retain all ownership rights to the copyright of the thesis. I also retain the right to use in future works (such as articles or books) all or part of this thesis.

Vincent Vartabedian

April 13, 2015

**Development of a Tumor Membrane-based Vaccine for Breast Cancer, Studied as a  
Monotherapy and in Combination with Immune Checkpoint Blockade Antibodies**

by

Vincent F. Vartabedian

Periasamy Selvaraj, Ph.D.  
Adviser

Department of Biology

Periasamy Selvaraj, Ph.D.  
Adviser

Chris Beck, Ph.D.  
Committee Member

Gregg Orloff, Ph.D.  
Committee Member

2015

**Development of a Tumor Membrane-based Vaccine for Breast Cancer, Studied as a  
Monotherapy and in Combination with Immune Checkpoint Blockade Antibodies**

By

Vincent F. Vartabedian

Periasamy Selvaraj, Ph.D.

Adviser

An abstract of  
a thesis submitted to the Faculty of Emory College of Arts and Sciences  
of Emory University in partial fulfillment  
of the requirements of the degree of  
Bachelor of Sciences with Honors

Department of Biology

2015

## **Abstract**

### **Development of a Tumor Membrane-based Vaccine for Breast Cancer, Studied as a Monotherapy and in Combination with Immune Checkpoint Blockade Antibodies**

By

Vincent F. Vartabedian

1 in 8 women will be diagnosed with breast cancer in her lifetime, and the five year survival rate for patients diagnosed with stage III or IV breast cancer is only 25%, due to metastasis. Chemotherapy serves as the primary standard of care to treat metastatic growth. However, chemotherapy can cause severe side effects due to its non-specific nature, and, likely due to inter-personal and intra-tumoral heterogeneity, its efficacy is lacking. Here, we propose the use of a personalized tumor membrane vesicle (TMV) based vaccine made from autologous tumor cells and decorated with GPI-anchored IL-12 and B7-1 via a simple protein transfer method, and we evaluate its efficacy alone and in combination with immune checkpoint blockade antibodies against CTLA-4 and PD-L1 in 4TO7 and E0771 breast cancer settings. We show that our modified TMV vaccine reduces tumor burden as a monotherapy in the 4TO7 system, but do not find statistically significant differences in efficacy in either combination therapy setting. Perhaps due to immune checkpoint upregulation, we do not see efficacy of our vaccine in the E0771 setting.

**Development of a Tumor Membrane-based Vaccine for Breast Cancer, Studied as a  
Monotherapy and in Combination with Immune Checkpoint Blockade Antibodies**

By

Vincent F. Vartabedian

Periasamy Selvaraj, Ph.D.

Adviser

A thesis submitted to the Faculty of Emory College of Arts and Sciences  
of Emory University in partial fulfillment  
of the requirements of the degree of  
Bachelor of Sciences with Honors

Department of Biology

2015

### **Acknowledgements**

First, I would like to thank Dr. Selvaraj for his guidance, support, and friendship for the past 3.5 years. I would not be the scientist I am today without him. Furthermore, I would also like to thank my graduate mentor, Jaina Patel, Ph.D. for keeping me on track and helping me throughout my time in the lab. Furthermore, Erica Bozeman, Ph.D. and Chris Pack, Ph.D. also provided key mentorship. Finally, I would like to thank my committee members, Chris Beck, Ph.D. and Gregg Orloff, Ph.D. for their assistance with this thesis.

## **Table of Contents**

Abbreviations Used .....	1
Introduction .....	2
Materials and Methods .....	10
Results .....	18
Discussion .....	35
Financial & competing interest disclosure .....	41
Appendix A: Publications .....	42
References .....	45

**Tables and Figures**

Table 1 .....	6
Figure .....	18
Table 2 .....	16
Table 3 .....	17
Figure 2 .....	18
Figure 3 .....	19
Figure 4 .....	20
Figure 5 .....	21
Figure 6 .....	22
Figure 7 .....	23
Figure 8 .....	24
Figure 9 .....	25
Figure 10 .....	27
Figure 11 .....	28
Figure 12 .....	29
Figure 13 .....	30
Figure 14 .....	31
Figure 15 .....	32
Figure 16 .....	33
Figure 17 .....	34
Figure 18 .....	36

**Abbreviations used**

APC, antigen presenting cell

CAR T cell, chimeric antigen receptor T cell

CTLA-4, cytotoxic T lymphocyte associated protein-4

DC, dendritic cell

FACS, florescence activated cell sorting

GPI, glycosyl-phosphatidylinositol

IFN, interferon

IL, interleukin

ISM, immunostimulatory molecule

MDR, multi-drug resistance

MFI, mean florescence intensity

PD-L1, programmed death-ligand 1

RBCs, red blood cells

TMV, tumor membrane vesicle

## **Introduction**

About 1.6 million Americans were diagnosed with cancer in 2014, with about 600,000 dying from the disease, making it the cause of one out of every four American deaths, and the leading cause of death among Americans aged between 40 and 79 [1]. Among females, breast cancer was the most diagnosed; 1 in 8 women will be diagnosed during her lifetime, and, in 2014, breast cancer accounted for about 230,000 new cancer cases (28% of all female diagnoses) and 40,000 deaths (15% of all female cancer deaths) [1].

Due to improvements in overall treatment and detection methods, the number of deaths per year due to breast cancer has been slowly decreasing [2, 3]. However, side effects and other clinical challenges of common therapies limit their overall efficacy.

Generally, breast cancer treatment is broken down into two parts: local and systemic. Local therapy aims to eliminate cancer cells at the primary tumor site. Local therapy usually includes surgical excision of the tumor and radiation. A 20-year trial has shown that such local therapies are effective at treating early stage (I and II) breast cancers (breast cancers that have not detectably spread past the axillary lymph nodes) [4]. Similarly, an 8-year study showed that local therapy was sufficient for treating breast cancer and metastasis in patients with low-grade (T1 or T2) tumors, with high five-year survival rates [5].

However, survival results are not as satisfactory for patients with later (III or IV) stage breast cancer, and the 20-year study also revealed that about 25% of patients had distant recurrence at some point after local therapy, despite initial efficacy [4]. According to the NCI's SEER database (*seer.cancer.gov*), 5-year survival for patients with distant metastasis (meaning that

the cancer has moved from its primary site to other areas of the body, including lymph nodes, the brain, and bones) is a paltry 25%, demonstrating the importance of therapies to combat metastasis.

Systemic therapies are full-body therapies that aim to target cancer cells anywhere in the body, thus preventing this high mortality rate due to metastasis. The most common form of systemic therapy is chemotherapy. However, chemotherapy has side effects such as reduction of white blood cells, reduction of platelets, anemia, fever, hair loss, neurologic symptoms, renal symptoms, and gastrointestinal symptoms that can strongly negatively impact quality of life both during and after treatment [6]. More importantly, these side effects are not outbalanced by overall chemotherapy efficacy. For example, a large phase III trial showed that median survival rates of patients with metastatic breast cancer treated with doxorubicin, paclitaxel, or both was only about 19 months for patients taking doxorubicin, about 22 months for patients taking paclitaxel, and 22 months for patients taking both, and the overall five-year survival rate across all three treatments was only about 13% [7].

The intrinsic heterogeneity of cancer cells is often attributed as a key reason for chemotherapy's underwhelming efficacy [8, 9]. For example, although some subset of breast cancer cells are susceptible to chemotherapy, some tumorigenic breast cancer cells have intrinsic resistance to chemotherapy [10]. Additionally, differential gene expression, especially of Multi-Drug Resistance (MDR) genes, is another source of heterogeneity attributed to the differential response to chemotherapy [11]. These resistant cells can then be selected for with chemotherapy, lay dormant, then re-emerge and spread, more difficult to treat than before [12].

For these reasons and others, the need for new systemic treatments is clear. In particular, treatments that are more specific to each patient's cancer, yield greater anti-metastatic effects, and have less side effects are of highest necessity. Cancer immunotherapies hold this promise.

Cancer immunotherapies (summarized in Table 1) have recently entered the spotlight with the recent approval (or clinical trials) and success of therapies such as interleukin-2 (IL-2), interferon-alpha (IFN- $\alpha$ ), ipilimumab (anti-CTLA-4 antibody; trade name: Yervoy<sup>®</sup>), nivolumab (anti-PD-1 antibody; trade name: Opdivo<sup>®</sup>), MPDL3280A (anti-PD-L1 antibody), sipuleucel-T (trade name: Provenge<sup>®</sup>), and chimeric antigen T cell therapy.

IL-2, IFN- $\alpha$ , ipilimumab, and nivolumab are passive immunotherapies: therapies that cause general immune system activation or block immune system checkpoints without causing a specific immune response.

IL-2 and IFN- $\alpha$  are both signaling molecules that cause general immune system upregulation. A large meta-analysis showed that IL-2, a cytokine that regulates lymphocytes, has shown efficacy in treating metastatic melanoma, especially in certain patient subsets [13]. Similarly, in another large meta-analysis, IFN- $\alpha$ , an immune system-activating signaling molecule, has been shown to cause statistically significant benefits for systemically treating melanoma, including a statistically significant reduction in death risk [14].

Ipilimumab and nivolumab are both antibodies that block immune system "off-switches." One of the two "emerging hallmarks" of cancer is "avoiding immune destruction," [15] and both antibodies block immune de-activation pathways.

Ipilimumab is a fully human monoclonal antibody approved in 2011 for late-stage melanoma treatment. It has been shown to extend melanoma survival rates by an average of ten months by binding to CTLA-4, an “off-switch” for T cells expressed on their surface, preventing cytotoxic T-cell inactivation and thus increasing their antitumor efficacy [16]. Twenty-four percent of patients treated with ipilimumab survived for two years or more. In addition to its efficacy, it also has much less severe side effects, including fatigue and skin rash, and only 12.9 percent of patients experience severe side effects [16].

Nivolumab, an antibody against programmed death 1 (PD-1), another T cell “off switch,” yields similar results. When given to patients with advanced melanoma, the therapy yielded 31% objective tumor regression, with little toxicity [17]. When the two antibodies were given in combination, 53% of patients saw an objective response, with only 18% having grade 3 or 4 adverse side effects [18].

The anti-PD-L1 is the newest checkpoint blockade antibody, and it is currently in clinical trials, with promising results. For example, it has been shown that the antibody can produce durable tumor regression and prolonged disease stabilization in patients with various types of cancer [19]. Further, only 9% of patients experienced grade 3 or 4 adverse side effects [19].

Sipuleucel-T differs from the previous immunotherapies in that it is an active cellular immunotherapy: it activates the immune system directly by stimulating a patient’s own dendritic cells to present PAP, a protein only expressed on prostate cancer cells. This is done by exposing a patient’s own dendritic cells to a recombinant fusion protein consisting of PAP fused

to granulocyte-macrophage colony-stimulating factor (GM-CSF), an activator of immune cells [20]. One clinical trial showed a relative reduction in death risk of 41% [20].

Another active immunotherapy that is gaining attention is that of using chimeric antigen receptor (CAR) T cells to treat cancer. Recently, one study showed that, in refractory B-ALL patients, 19-28z CAR T cell therapy yielded an 88% complete response rate [21]. It is hypothesized that combining this therapy with passive therapies such as ipilimumab or nivolumab can further increase its efficacy, but, as a monotherapy, it seems to be highly effective at fighting cancers with known antigens [22].

Table 1: Summary of the current status of numerous cancer immunotherapies.

Therapy	Company (trade name, if applicable)	Mechanism of action	Approval status
Sipuleucel-T	Dendreon (Provenge®)	Activate immune system against PAP, a protein expressed only on prostate cancer cells	FDA approved for prostate cancer
Ipilimumab (Anti-CTLA-4 antibody)	Bristol-Myers Squibb (Yervoy®)	Block CTLA-4, a T cell "off switch"	FDA approved for melanoma
Nivolumab (Anti-PD-1 antibody)	Bristol-Myers Squibb (Opdivo®)	Block PD-1, a T cell "off switch"	FDA approved for melanoma and non-small cell lung cancer
Anti-PD-L1 antibody	Genentech (MPDL3280A)	Block PD-L1, a T cell "off switch"	Clinical trials for bladder and non-small cell lung cancer

Additionally, other labs have achieved success at inducing immune system responses to cancer cells via DNA vaccines [23], tumor-derived heat shock protein vaccines [24], and tumor hybrid cell vaccines [25]. Coming off of the promise and efficacy of these immunotherapies, we

describe a method for creating a novel therapeutic cancer immunotherapy vaccine and show its efficacy in certain breast cancer systems.

Our lab has proposed the use of a tumor membrane-based cancer vaccine created by decorating tumor-derived cell membrane vesicles with cytokines and other immunostimulatory molecules (ISMs) anchored by glycosyl-phosphatidylinositol (GPI).

Previously, we have shown that the GPI-anchor, a glycolipid commonly found as an anchor for naturally produced proteins [26], can easily be attached post-translationally to the C-terminus of immunostimulatory proteins B7-1 and IL-12 using recombinant DNA techniques, without either proteins' functionality being affected [27, 28]. Such GPI-linked proteins can then be purified from cells and incubated with live cells or cell membrane vesicles to incorporate the protein to the surface of the cell or membrane, a procedure known as protein transfer [27, 29] (Figure 1).

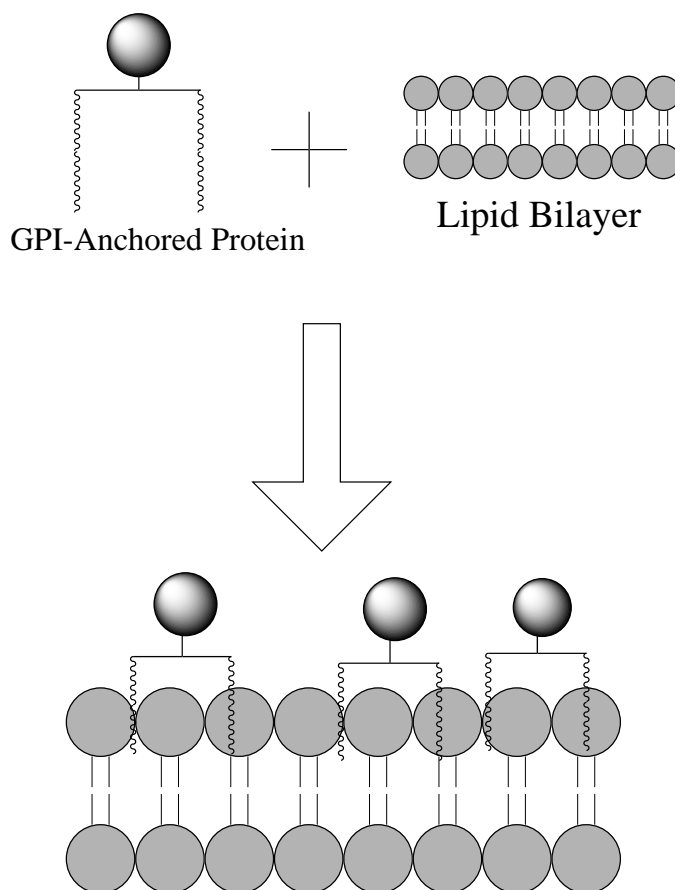


Figure 1: A simple schematic of our GPI-dependent protein transfer method. Adapted from Patel JM, **Vartabedian VF**, Selvaraj P. Lipid-mediated Cell Surface Engineering. Micro- and Nano Engineering of the Cell Surface 2014; Chapter 6: Pages 121-141 (ISBN: 978-1-4557-3146-6). (Edited by Weian Zhao and Jeffrey M. Karp, Elsevier Publications). [?](#)

Previously, our lab has shown that tumor membranes decorated with B7-1 [29], IL-12 [28], or both [30] and used as a vaccine cause an immune response against the cancer from which the membranes are derived, and other studies confirm that these two proteins can work synergistically to combat tumors [31-36]. The benefit of this therapy is that it is autologous (personalized) for each cancer: all of the intratumoral and interpersonal heterogeneity of the tumor tissue in a patient is included in the patient-specific vaccine [37]. Overall, we think that this novel vaccination approach should allow for efficacy despite problems typically caused by tumor heterogeneity.

In the current study, we attempt to confirm this hypothesis with two breast cancer cell lines. We also attempt to improve our vaccine's efficacy by combining the decorated TMV vaccine with checkpoint blockade antibodies against CTLA-4 and PD-L1. Because our vaccine causes an immune response that may be dampened by such immune checkpoints, we believe that this combination therapy approach should increase our vaccine's efficacy. Furthermore, we think that the added immune signaling will work better than either monotherapy approach because multiple pathways will be affected.

## **Materials and Methods**

### **Animals, Antibodies, and Cell Lines**

Six to eight week-old female BALB/c and C57BL/6J mice were purchased from Jackson Laboratory. All experiments were conducted in accordance with Emory University IACUC guidelines. CHO-K1 cell transfectants expressing either GPI-mIL-12 or GPI-mB7-1-short were maintained in RPMI 1640 and 5% Bovine Calf Serum (Sigma Aldrich) containing 10 µg/ml Blasticidin (Invitrogen).

4T07 cells are a spontaneous, aggressive, non-metastatic Balb/c/c3H mammary-derived cancer cell line [38]. E0771 cells, a spontaneous, metastatic C57BL/6 breast adenocarcinoma-derived cancer cell line [39] derived by Francis M. Sirotnak (Sloan-Kettering Institute) [40] were a kind gift from Subra Malarkannan (The Medical College of Wisconsin).

FITC-conjugated goat-anti-mouse IgG and FITC-conjugated goat-anti-rat IgG (Jackson Immunoresearch) were used for flow cytometry analysis.

### **GPI-ISM DNA Constructs**

As described by Patel et al. (submitted to Biomaterials) via an EcoRI restriction enzyme site, mouse GPI-B7-1 was constructed by attaching the CD59 GPI-signal sequence nucleotides to the extracellular domain of mouse B7-1 (GenBank BC131959.1, nucleotides 45-800). To remove an internal trypsin cleavage site, a K253A mutation was inserted by changing nucleotides AAG to GCG. To construct mouse GPI-IL-12, the CD59 GPI-signal sequence was attached to the p35 subunit of mouse IL-12. This sequence was then followed by an IRES along with the soluble p40 subunit of mouse IL-12. Both constructs were inserted in a pUB6<sup>blast</sup> vector (Invitrogen).

### **Purification and Quantification of GPI-ISMs**

Cell pellets of CHO-K1 cell transfectants expressing GPI-mIL-12 or GPI-B7-1 were lysed with continual stirring for 4 h at 4°C with a buffer composed of 50 mM Tris-HCL pH 8, 2% n-octyl-β-D-glucopyranoside (A.G. Scientific), 20 mM iodoacetate, 5 mM EDTA, 1mM zinc chloride, 1:100 dilution of Protease Inhibitor Cocktail (Sigma), and 2 mM PMSF. The lysate was then centrifuged at 15,000 RPM using a JA-20 rotor (Beckman) for 1 h at 4°C. After centrifugation, the supernatant was passed through a 70 μm cell strainer to remove remaining cell debris.

Affinity chromatography was used to purify the GPI-ISMs from the lysate. First, lysate was passed through a Sepharose 4B bead (Sigma-Aldrich) pre-column. Lysate from CHO-K1 cells expressing GPI-mIL-12 was then passed through an immunoaffinity column consisting of sepharose beads coupled to rat antibody C17.8 (anti-mIL-12 p40). Lysate from CHO-K1 cells expressing GPI-mB7-1 was passed through an immunoaffinity column consisting of Sepharose beads coupled to 1G10.

To remove contaminating proteins before eluting each GPI-ISM, each affinity column was washed with a buffer of 50 mM Tris-HCL pH8, 1% Triton X-100, 200 mM NaCL, and 10 mM iodoacetate, then with a buffer of 20 mM Tris-HCL pH 7.5, 0.1% n-octyl-β-D-glucopyranoside, and 10 mM iodoacetate.

GPI-mIL-12 was then eluted with a buffer of pH 2.8 consisting of 100 mM glycine-HCL, 1% n-octyl-β-D-glucopyranoside, and 10 mM iodoacetate. GPI-B7-1 was eluted with a buffer of pH 11.6 consisting of 100 mM triethylamine, 1% n-octyl-β-D-glucopyranoside, and 10 mM

iodoacetate. Samples from eluted fractions were analyzed by SDS-PAGE, then analyzed for presence and purity by western blot and silver staining. Protein-containing fractions were then combined in a 10-14 kDa MWCO dialysis bag (Fisherbrand) and concentrated using polyvinylpyrrolidone (Sigma-Aldrich). After concentration, the proteins were dialyzed with a buffer of 500 ml PBS supplemented with 0.05% n-octyl- $\beta$ -D-glucopyranoside. The buffer was exchanged 3 times and the dialyzed GPI-ISM sample was then stored at 4°C.

GPI-ISMs were quantified using a micro BCA kit (Thermo Scientific).

### **Protein Transfer of GPI-ISMs onto Sheep Red Blood Cells**

In order to confirm the ability of purified GPI-ISMs to incorporate onto cell membranes, each GPI-ISM was protein transferred onto sheep red blood cells (RBCs) (HemoStat Laboratories). First, each GPI-ISM was centrifuged at 13,200 RPM for 1 h at 4°C in a micro-centrifuge (Eppendorf Centrifuge 5415 D). While the centrifugation was occurring, RBCs were washed in PBS, then resuspended in PBS fortified with 0.1% ovalbumin. RBCs were then counted using a hemocytometer and diluted to  $10 \times 10^6$  cells/ml in PBS/0.01% ovalbumin. 200  $\mu$ l of RBCs were then combined with 10  $\mu$ l of either GPI-ISM. Samples were then rotated end-over-end for 4 h at 37°C. Next, samples were placed in 1ml FACS buffer (PBS fortified with 1% Bovine Calf Serum [Sigma Aldrich] and 5 mM EDTA and centrifuged at 2000 RPM for 5 min at 4°C (Eppendorf Centrifuge 5810 R). The supernatant was aspirated, and the pellet was resuspended in 100  $\mu$ l FACS buffer before being analyzed by flow cytometry using anti-mIL-12 p40 rat antibody C17.8 as the primary antibody to detect levels of mIL-12 incorporation and 1G10 as the primary antibody to detect levels of mB7-1 incorporation before being incubated with FITC conjugated

goat anti-rat antibody [Jackson ImmunoResearch]. Samples were analyzed using a Dickinson and Company FACSCalibur flow cytometer, and results were analyzed using FlowJo.

### **Preparation and Quantification of Tumor Membrane Vesicles (TMVs) From 4TO7-RG or E0771**

#### **Tumor Tissue**

4TO7-RG or E0771 tumor tissue was isolated from mice inoculated with 400,000 cultured 4TO7-RG or E0771 and stored at -80°C. Before TMV preparation, samples were thawed in an ice bath. After thawing, the tissue was minced with dissection scissors and combined with a homogenization buffer consisting of 20 mM Tris-HCl pH 8.0, 10 mM NaCl, 0.1 mM MgCl<sub>2</sub>, and 0.1 mM PMSF. Samples were subjected to 4 rounds of homogenization, with each round consisting of 8 sec of active homogenization followed by 1 min of cooling on ice. Samples were then centrifuged at 1200 RPM for 5 minutes (Eppendorf Centrifuge 5810 R). The supernatant was collected, then pellets were suspended with homogenization buffer before being subjected to 4 more rounds of homogenization. The homogenate was again centrifuged, and the supernatant was collected again. The collected supernatant was pooled then passed through a BD Falcon nylon cell strainer before being distributed between 6 ultracentrifuge tubes. A 41% sucrose solution was then underlaid beneath the supernatant. These samples were ultracentrifuged for 1 h at 4°C using a SW41 Ti rotor at 23,000 RPM. After centrifugation, TMVs were harvested from the interphase. TMVs were then centrifuged at 14,000 RPM for 1 h at 4°C (Eppendorf Centrifuge 5415 D). Supernatant was discarded, then, to wash out remaining sucrose, TMVs were suspended with 1 ml PBS before being centrifuged again at 14,000 RPM for 1 h at 4°C (Eppendorf Centrifuge 5415 D). The TMV pellet was then resuspended in 1 ml PBS for storage at 4°C. TMVs were quantified using a micro BCA kit (Thermo Scientific).

### **Protein Transfer of GPI-ISMs onto 4TO7 or E0771 TMVs**

Protein transfer of GPI-mIL-12 and GPI-B7-1 onto 4TO7 TMVs was performed in 1.2 mL Eppendorf tubes using a ratio of 25  $\mu$ g of each GPI-ISM : 500  $\mu$ g TMV, with a total volume of 1 mL per tube. To serve as a control, one group of TMVs was put through the protein transfer process sans GPI-ISMs. First, each GPI-ISM was centrifuged at 13,200 RPM for 1 h at 4°C (Eppendorf Centrifuge 5415 D). Next, TMVs and GPI-ISMs were combined as per the above ratio, and both groups were rotated end-over-end for 4 h at 37°C. After rotating, samples were centrifuged at 13,200 RPM for 1 h at 4°C (Eppendorf Centrifuge 5415 D). After centrifugation, the supernatant was removed, and the samples were combined with PBS. Samples were centrifuged again at 13,200 RPM for 1 h at 4°C (Eppendorf Centrifuge 5415 D) to wash off any non-incorporated GPI-ISMs. Supernatant was discarded, then TMVs were resuspended in PBS.

### **Confirmation of Protein Transfer of GPI-ISMs onto 4TO7 or E0771 TMVs**

Flow cytometry was used to confirm the protein transfer of GPI-ISMs onto 4TO7 TMVs. A sample of protein transferred and mock protein transferred TMVs were first incubated with rat antibody C17.8 (anti-mIL-12 p40) or rat antibody 1G10 (anti-mB7-1) before being incubated with FITC-conjugated goat-anti-rat antibody [Jackson ImmunoResearch]. Samples were analyzed on a Dickinson and Company FACSCalibur flow cytometer, and results were analyzed using FlowJo.

### **Quantification of Protein Transferred TMVs**

Protein transferred and mock protein transferred TMVs were quantified using a micro BCA kit (Thermo Scientific).

### **Inoculation of BALB/c Mice with Live 4TO7 Cells**

4TO7 cells were maintained in DMEM (Corning CellGro) supplemented with 5% Bovine Calf Serum [Sigma Aldrich]. On the day of injection, 4TO7 cells were harvested via incubation with PBS supplemented with 5 mM EDTA. The cells were centrifuged at 1200 RPM for 5 min at 4°C (Eppendorf Centrifuge 5810 R), then the PBS/EDTA supernatant was discarded. To wash off remaining EDTA, the cell pellet was resuspended in PBS then centrifuged at 1200 RPM for 5 min at 4°C (Eppendorf Centrifuge 5810 R). Cell count and viability was calculated using trypan blue exclusion. Cells were diluted to 2,000,000 live cells / ml in PBS. 200,000 cells (100 µl) were injected into the hind flank of each mouse.

### **Therapeutic 4TO7 Combination Therapy Vaccination Strategy**

3 days post live cell injection, mice (n = 5) were treated according to the following schedule. All subcutaneous injections were performed on the opposite rear flank as the live cell inoculation, and treatments are summarized in Table 2. Group 1 was treated with PBS subcutaneously and PBS intraperitoneally. Group 2 was treated with mock protein transferred TMVs subcutaneously and PBS intraperitoneally. Group 3 was treated with protein transferred TMVs subcutaneously and PBS intraperitoneally. Group 4 was treated with protein transferred TMVs subcutaneously and anti-CTLA-4 antibody [9D9, Bio X Cell, 100 µg/mouse] intraperitoneally. Group 5 was treated with PBS subcutaneously and anti-CTLA-4 antibody [9D9, Bio X Cell, 100 µg/mouse] intraperitoneally. Group 6 was treated with protein transferred TMVs subcutaneously and anti-PD-L1 antibody [10F.92G, Bio X Cell, 100 µg/mouse] intraperitoneally. Group 7 was treated with

PBS subcutaneously and anti-PD-L1 antibody [10F.92G, Bio X Cell, 100 µg/mouse]

intraperitoneally. This treatment schedule was repeated 6 days post live cell injection.

Table 2: Vaccination schedule for 4TO7 therapeutic combination therapy experiment. Vaccinations were performed on day 3 post challenge and day 6 post challenge.

<b>Group</b>	<b>Subcutaneous</b>	<b>Intraperitoneal</b>
1 (5 mice)	PBS	PBS
2 (5 mice)	Unmodified TMVs (in PBS)	PBS
3 (5 mice)	GPI-mIL-12 + GPI-mB7-1 protein transferred TMVs (in PBS)	PBS
4 (5 mice)	GPI-mIL-12 + GPI-mB7-1 protein transferred TMVs (in PBS)	Anti-CTLA-4 antibody
5 (5 mice)	PBS	Anti-CTLA-4 antibody
6 (5 mice)	GPI-mIL-12 + GPI-mB7-1 protein transferred TMVs (in PBS)	Anti-PD-L1 antibody
7 (5 mice)	PBS	Anti-PD-L1 antibody

### **E0771 Prophylactic Vaccination Strategy**

It has been shown that, when compared to single doses or multiple, equal doses, increasing antigenic stimulation exponentially over a series of days can yield a stronger immune response [41]. Inspired by this, we administered exponentially increasing doses of PBS (vehicle), mock protein transferred E0771 TMVs, or E0771 TMVs protein transferred with GPI-mIL-12 and GPI-mB7-1 over the course of three days in concordance with Table 1.

Table 3: Vaccination schedule for E0771 prophylactic vaccination experiment.

Group	Day 0	Day 2	Day 4
1 (4 mice)	100 $\mu$ l PBS	100 $\mu$ l PBS	100 $\mu$ l PBS
2 (3 mice)	100 $\mu$ l PBS	100 $\mu$ l PBS	100 $\mu$ l PBS
3 (3 mice)	100 $\mu$ l 2.5 $\mu$ g /ml Mock PT'd TMVs (in PBS)	100 $\mu$ l 25 $\mu$ g /ml Mock PT'd TMVs (in PBS)	100 $\mu$ l 250 $\mu$ g /ml Mock PT'd TMVs (in PBS)
4 (3 mice)	100 $\mu$ l 2.5 $\mu$ g /ml PT'd TMVs (in PBS)	100 $\mu$ l 25 $\mu$ g /ml PT'd TMVs (in PBS)	100 $\mu$ l 250 $\mu$ g /ml PT'd TMVs (in PBS)
5 (3 mice)	100 $\mu$ l 5 $\mu$ g /ml Mock PT'd TMVs (in PBS)	100 $\mu$ l 50 $\mu$ g /ml Mock PT'd TMVs (in PBS)	100 $\mu$ l 500 $\mu$ g /ml Mock PT'd TMVs (in PBS)
6 (3 mice)	100 $\mu$ l 5 $\mu$ g /ml PT'd TMVs (in PBS)	100 $\mu$ l 50 $\mu$ g /ml PT'd TMVs (in PBS)	100 $\mu$ l 500 $\mu$ g /ml PT'd TMVs (in PBS)
7 (3 mice)	100 $\mu$ l 10 $\mu$ g /ml Mock PT'd TMVs (in PBS)	100 $\mu$ l 100 $\mu$ g /ml Mock PT'd TMVs (in PBS)	100 $\mu$ l 1000 $\mu$ g /ml Mock PT'd TMVs (in PBS)
8 (3 mice)	100 $\mu$ l 10 $\mu$ g /ml PT'd TMVs (in PBS)	100 $\mu$ l 100 $\mu$ g /ml PT'd TMVs (in PBS)	100 $\mu$ l 1000 $\mu$ g/ml PT'd TMVs (in PBS)

### Tumor Growth Tracking

Growth of all tumors was tracked every three to four days post live 4TO7 or E0771 cell injection using digital calipers (Pittsburgh). Tumor area was measured by multiplying tumor length and width.

### Statistical analysis

On GraphPad Prism, statistical two-way ANOVA with a post hoc Bonferroni test was used to determine statistical significance of tumor size differences. The Bonferroni post-test was used to generate P values at each time point. All error bars shown are SEM. For the sake of clarity, 4TO7 stats are divided across multiple figures, using the same control groups shown in Figure 7.

## Results

### **Purification of GPI-mIL-12**

CHO-K1 cells expressing GPI-anchored mIL-12 were lysed and purified with a Sepharose 4B bead pre-column followed by the affinity chromatography column consisting of Sepharose beads coupled to anti-mIL-12 antibody C17.8. Protein-containing fractions were determined via SDS PAGE followed by western blot (Figure 2) or silver stain (data not shown).

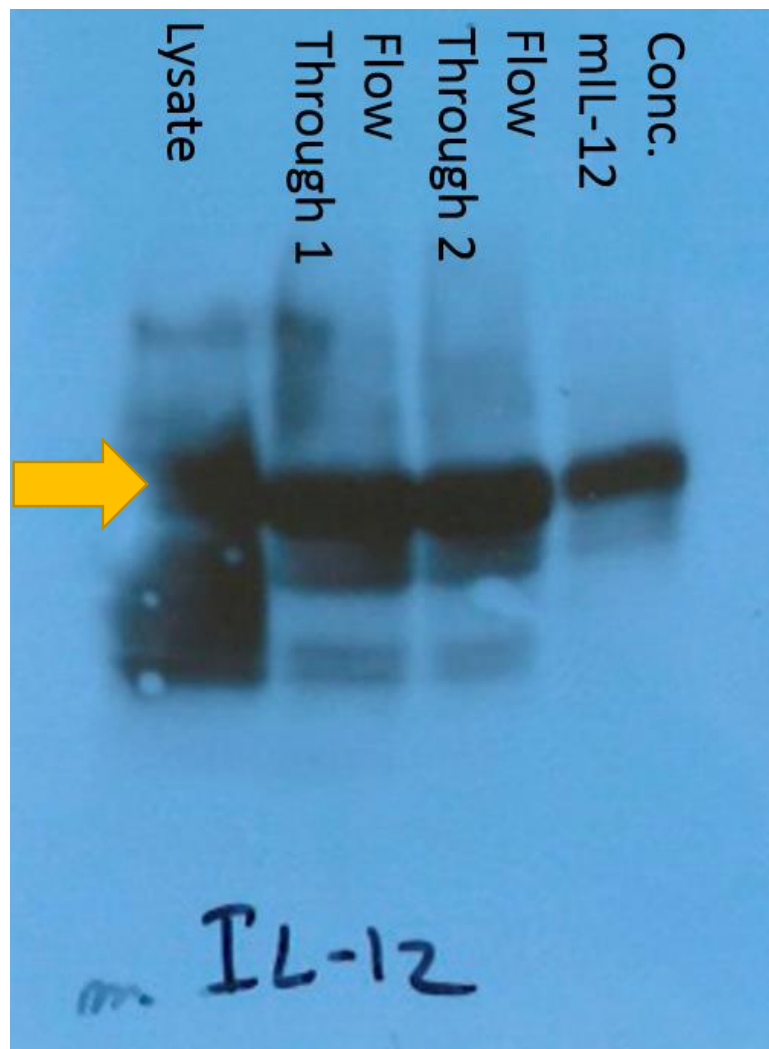


Figure 2: The presence of mIL-12 was detected in the purified concentrated fractions by SDS-PAGE followed by western blot.

### GPI-mIL-12 spontaneously incorporates onto the surface of sheep red blood cells

To test the ability of purified GPI-mIL-12 to spontaneously incorporate into cell membranes, GPI-mIL-12 was incubated with sheep red blood cells for 4 h at 37°C. Flow cytometry was then performed to detect the level of incorporation (Figure 3). The peak shift between the unstained and secondary-antibody-only peaks and the experimental peak suggests that the protein transfer was successful.

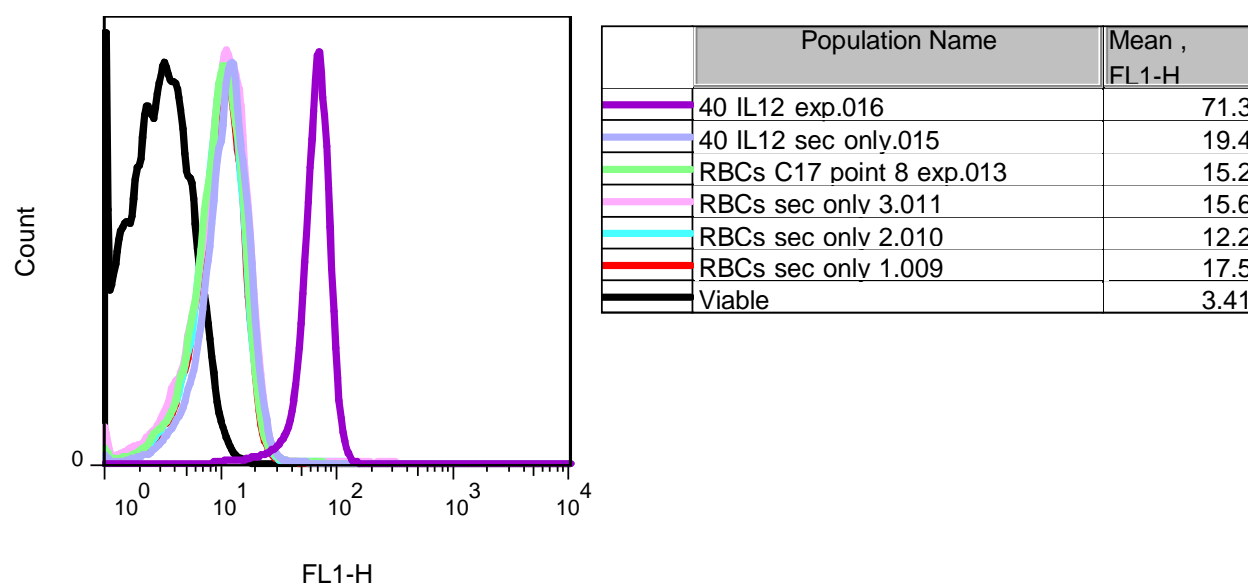


Figure 3: Flow cytometry data of GPI-mIL-12 incubated with sheep red blood cells (RBCs). The peak corresponding to the RBCs protein transferred with GPI-mIL-12 is shifted right compared to the unstained and secondary-only peaks, and the Mean FL1-H increased, suggesting that incorporation was successful.

### Purification of GPI-mB7-1

CHO-K1 cells expressing GPI-anchored mB7-1 were lysed, and GPI-mB7-1 was purified using the same experimental set up as above, using anti mB7-1 antibody 1G10 in place of anti-mIL-12 antibody C17.8. After column elution, protein-containing fractions were again determined via western blotting (Figure 4) and silver staining (data not shown). Those fractions were then combined and concentrated via polyvinylpyrrolidone concentration and dialysis.

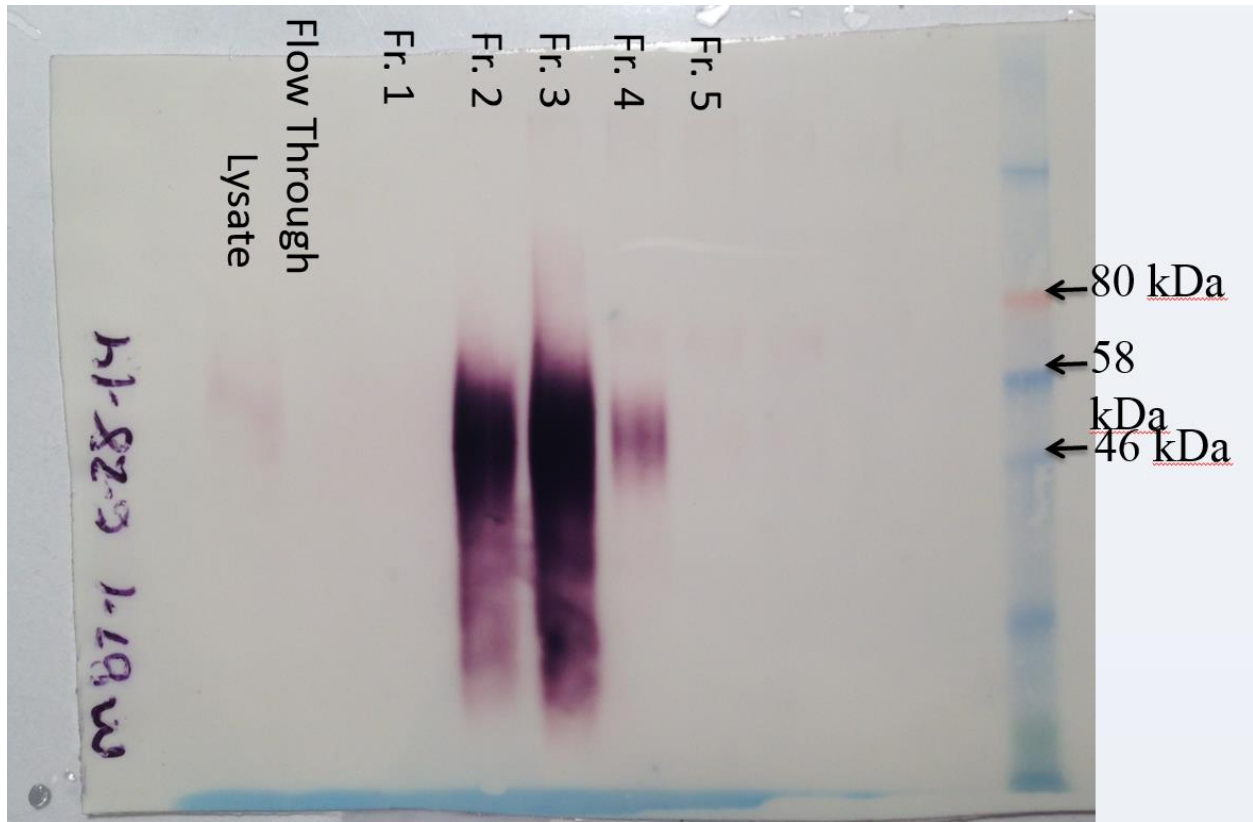


Figure 4: Western blot results using anti-mB7-1 primary antibody 1G10 show the presence of the GPI-mB7-1 in fractions 2, 3, and 4.

#### **GPI-mB7-1 spontaneously incorporates onto sheep RBCs**

To test the ability of the GPI-mB7-1 to spontaneously incorporate onto cell membranes, purified GPI-mB7-1 was incubated with sheep red blood cells for 4 h at 37° C at three different concentrations (5  $\mu$ g, 10  $\mu$ g, and 25  $\mu$ g). Flow cytometry was then performed to detect the level of incorporation (Figure 5). The peak shift between the unstained and secondary-antibody-only peaks and the experimental peak suggests that the protein transfer was successful and occurred in a concentration-dependent manner.

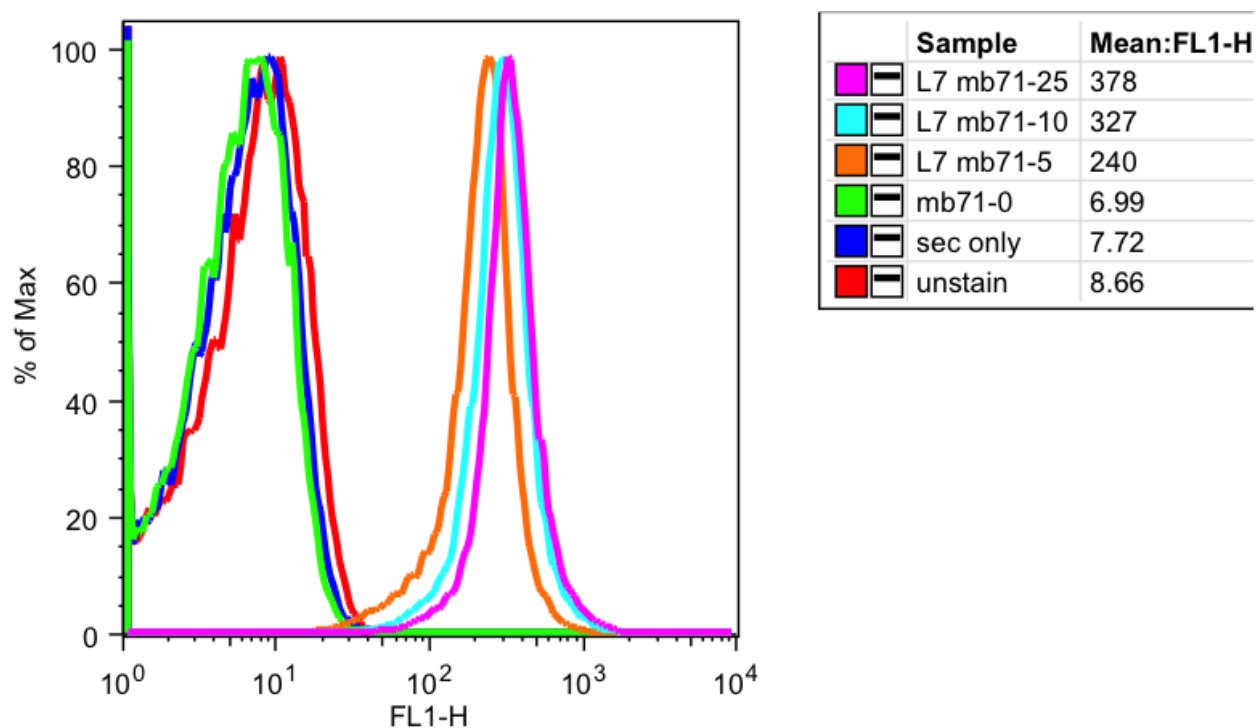


Figure 5: The peaks corresponding to the RBCs protein transferred with varying doses of GPI-mB7-1 is shifted right compared to the unstained and secondary-only peaks, and the MFI increased, suggesting that incorporation was successful. Furthermore, there is a rightward shift of each protein-transferred group, with a larger dose of GPI-mB7-1 yielding a larger rightward shift and corresponding MFI increase, suggesting that the incorporation is dose-dependent.

#### Homogenization of 2.94 g 4TO7-RG tumor tissue yields 16 mg TMVs

4TO7-RG tumor tissue previously harvested and stored at  $-80^{\circ}\text{C}$  was used to generate TMVs.

After homogenization and centrifugation over a 41% sucrose solution, TMVs were harvested from the interphase. Amount harvested was quantified with a BCA protein approximation kit.

Briefly, known concentrations of BSA were subjected to the kit, and a standard curve was created based upon the BSA samples' absorbances at 590 nm (Figure 6). From this curve, 16 mg of TMVs were found to have been generated at a concentration of 2.1 mg/ml.

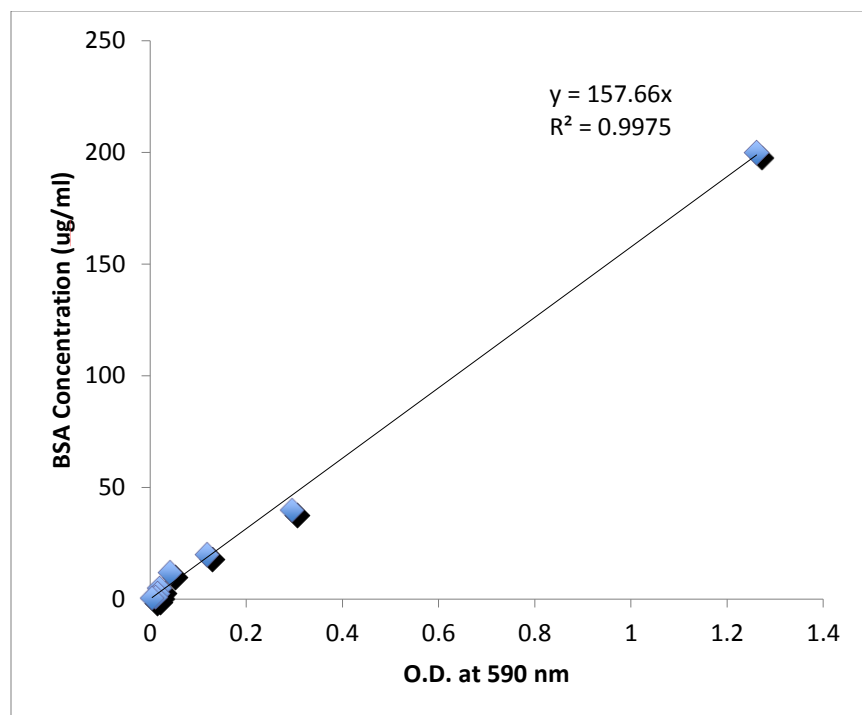


Figure 6: Standard curve generated via BCA protein approximation kit used to determine quantity and concentration of 4TO7-RG TMVs generated. 16 mg were generated from 2.94 g 4TO7-RG tumor tissue at a concentration of 2.1 mg/ml.

#### **Protein transfer of GPI-mB7-1 and GPI-mIL-12 onto 4TO7-RG TMVs**

GPI-mIL-12 and GPI-mB7-1 were incubated with 4TO7 TMVs for four hours at 37° C on an end-over-end rotator as described under methods.

#### **Therapeutic vaccination with protein-transferred (GPI-mIL-12 and GPI-mB7-1) TMVs induces protection against 4TO7 tumor challenge**

To determine if TMVs modified with GPI-mIL-12 and GPI-mB7-1 had any effect on tumor growth, mice were therapeutically vaccinated with PBS (control), unmodified TMVs, or TMVs modified with GPI-mIL-12 and GPI-mB7-1 after being inoculated with 4TO7RG tumor cells.

Tumor growth was then tracked for 40 days post-challenge (Figure 7), and statistical significance in growth difference was determined via two-way ANOVA. No statistically

significant difference in growth was seen between PBS-vaccinated and unmodified TMV-vaccinated groups across all time points ( $P > 0.05$ ). Although there initially was no difference in tumor growth between all three groups, at day 36 post-challenge, tumor burden of mice vaccinated with modified TMVs began to be statistically significantly smaller ( $P < 0.05$ ). This difference became more significant ( $P < 0.01$ ) at day 40, and highly significant ( $P < 0.001$ ) from day 43 to day 50. Overall, these results suggest that 4TO7 tumor burden can be reduced by therapeutic vaccination with 4TO7 TMVs modified with GPI-mIL-12 and GPI-mB7-1. For the sake of clarity, stats are divided across multiple figures, using the same control groups shown in Figure 7. Additionally, all mice were tumor free on day zero post-challenge, and all mice had measurable tumors beginning day three post-challenge.

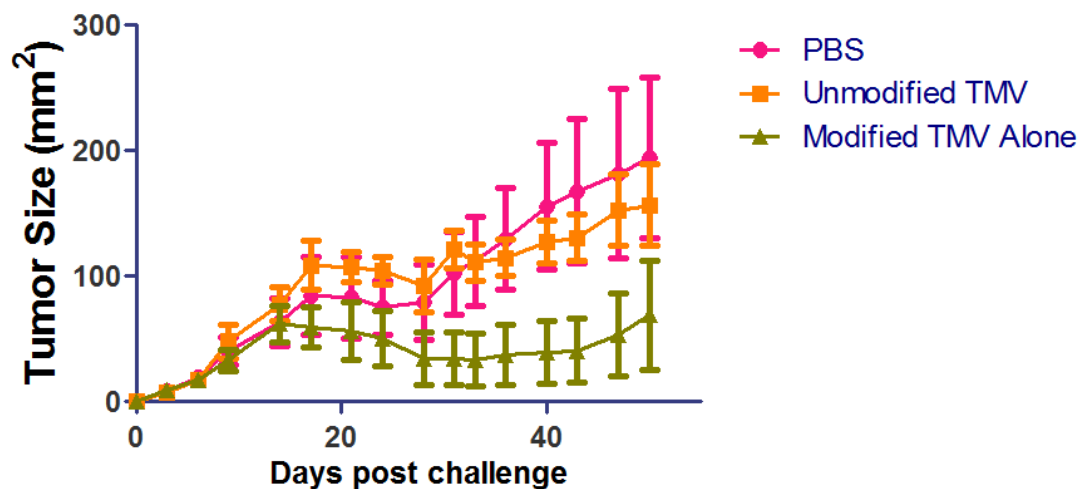


Figure 7: Therapeutic vaccination of mice (for each group,  $n=5$ .) with GPI-mIL-12 + GPI-mB7-1 protein transferred-4TO7 TMVs delays 4TO7-RG tumor growth as shown by comparison of average 4TO7-RG tumor size of mice vaccinated with PBS (control), unmodified TMVs, or TMVs modified with GPI-mIL-12 and GPI-mB7-1. There was no statistically significant difference in average tumor size between mice vaccinated with PBS and mice vaccinated with unmodified TMV across all time points. The size difference induced by vaccination with GPI-mIL-12 + GPI-

mB7-1 modified TMVs becomes statistically significant on day 36 and continues until the experimental endpoint.

### Combination therapy of anti-CTLA-4 antibody and GPI-mIL-12 + GPI-mB7-1 protein

transferred-4TO7 TMVs modified with GPI-mIL-12 and GPI-mB7-1 yields statistically insignificantly smaller 4TO7 tumors than either therapy alone

We also administered our vaccine consisting of TMVs modified with GPI-mIL-12 and GPI-mB7-1 in a combination setting, combining it with anti-CTLA-4 antibody. All three therapies yielded statistically smaller tumors than vaccination with PBS (vehicle) or unmodified TMVs. Anti-CTLA-4 antibody monotherapy yielded statistically significantly smaller tumors at day 36 ( $P < 0.05$ ). Starting on day 40 and continuing to day 43, this difference became more statistically significant ( $P < 0.01$ ) tumors, and, on days 47 and 50, it became highly statistically significant ( $P < 0.001$ ) (Figure 8).

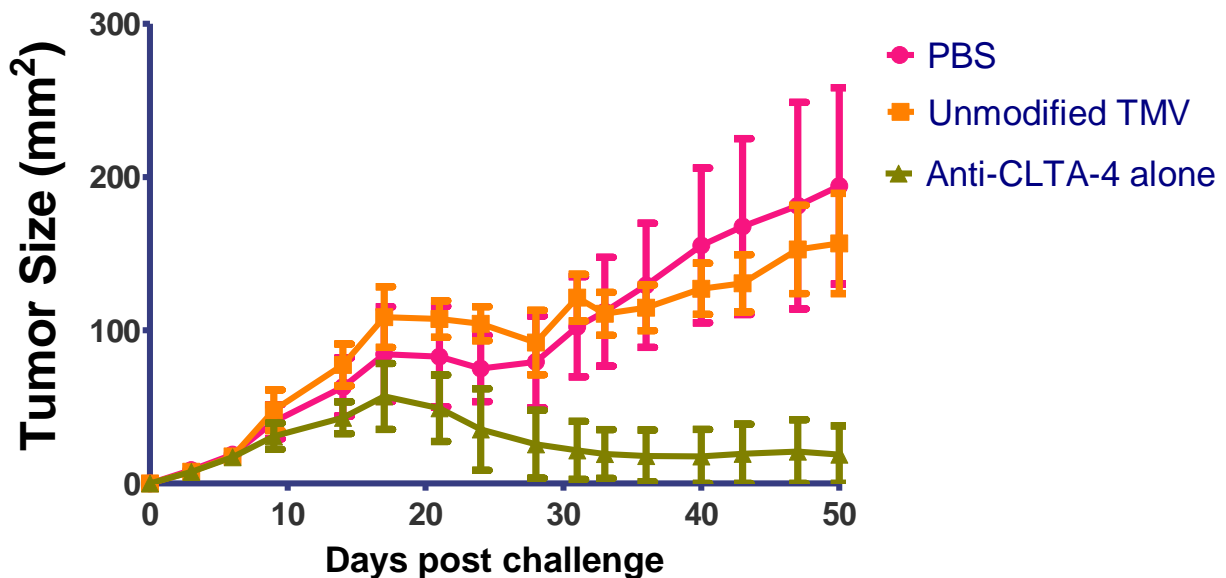


Figure 8: Injection of mice (for each group, n=5.) with anti-CTLA-4 antibody yields average smaller tumors than injection with PBS or unmodified TMVs as shown by comparison of

average 4T07 tumor size of mice treated with PBS, unmodified TMVs, or anti-CTLA-4 alone. The size difference becomes statistically significant on day 36 and continues until the experimental endpoint.

Modified TMV and anti-CTLA-4 combination therapy yielded very similar results, with tumors being statistically significantly smaller than PBS-treated mice at days 31 and 33 ( $P < 0.05$ ), becoming more significant ( $P < 0.01$ ) at day 36, and becoming highly significant at days 40, 43, 47, and 50 ( $P < 0.001$ ) (Figure 9).

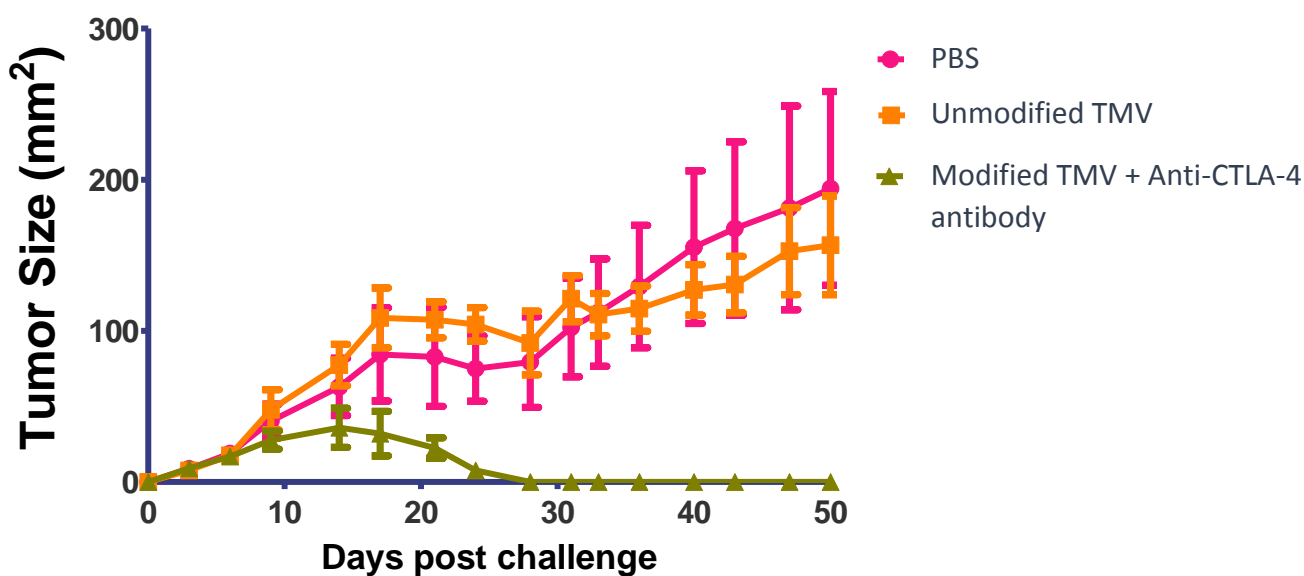


Figure 9: Treatment of mice (for each group,  $n=5$ .) with TMVs modified with GPI-mIL-12 + GPI-mB7-1 and anti-CTLA-4 antibody yields average smaller tumors than injection with PBS or unmodified TMVs as shown by comparison of average 4T07 tumor size of mice treated with PBS, unmodified TMV, or TMVs modified with GPI-mIL-12 and GPI-mB7-1 and anti-CTLA-4 antibody. Tumor size becomes significantly smaller at day 31 (note that, although the tumors appear to regress to an average size of  $0 \text{ mm}^2$ , they are merely approaching  $0 \text{ mm}^2$ ).

Both monotherapies were compared with the combination therapy by tracking average tumor size of treated mice (Figure 10). When comparing both monotherapies to each other, there was

no statistically significant difference in average tumor size ( $P > 0.05$ ). Although anti-CTLA-4 monotherapy yielded smaller tumors than modified TMV monotherapy, this size difference was not statistically significant ( $P > 0.05$ ). Similarly, although the combination therapy yielded smaller average tumor size than either monotherapy, the difference was not statistically significant ( $P > 0.05$ )

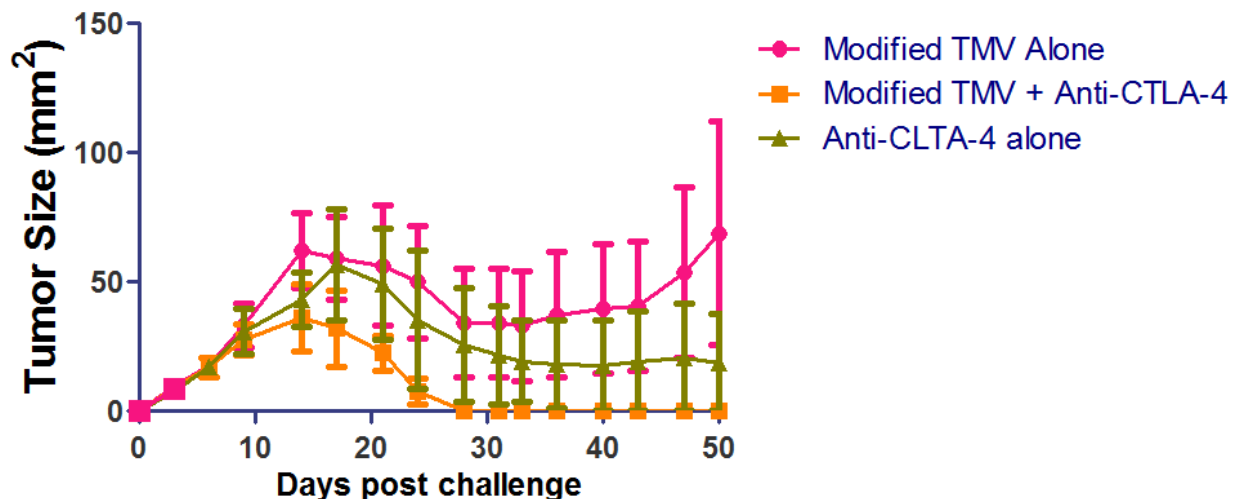


Figure 10: Treatment of mice (for each group, n=5.) with GPI-mIL-12 + GPI-mB7-1 modified TMVs alone, anti-CTLA-4 antibody alone, or combination therapy of both GPI-mIL-12 + GPI-mB7-1 modified TMVs and anti-CTLA-4 antibody yields statistically similar 4T07 tumor growth, as shown by comparison of average tumor size of mice treated with only TMVs modified with GPI-mIL-12 and GPI-mB7-1, only anti-CTLA-4 antibody, or both. There was no statistically significant difference between tumor sizes across all three groups ( $P > 0.05$ ).

**Combination therapy of anti-PD-L1 antibody and TMVs modified with GPI-mIL-12 and GPI-mB7-1 yields statistically insignificantly larger tumors than either therapy alone**

We also administered our vaccine consisting of TMVs modified with GPI-mIL-12 and GPI-mB7-1 in another combination therapy setting, combining it with anti-PD-L1 antibody. All three therapies yielded statistically smaller tumors than vaccination with PBS (control) or unmodified TMVs. Anti-PD-L1 treated mice, when compared to PBS-treated mice, had statistically significantly smaller tumors starting on day 36 ( $P < 0.05$ ), and this difference became more significant on days 40 and 43 ( $P < 0.01$ ). It became highly significant on days 47 and 50 ( $P < 0.001$ ) (Figure 11).

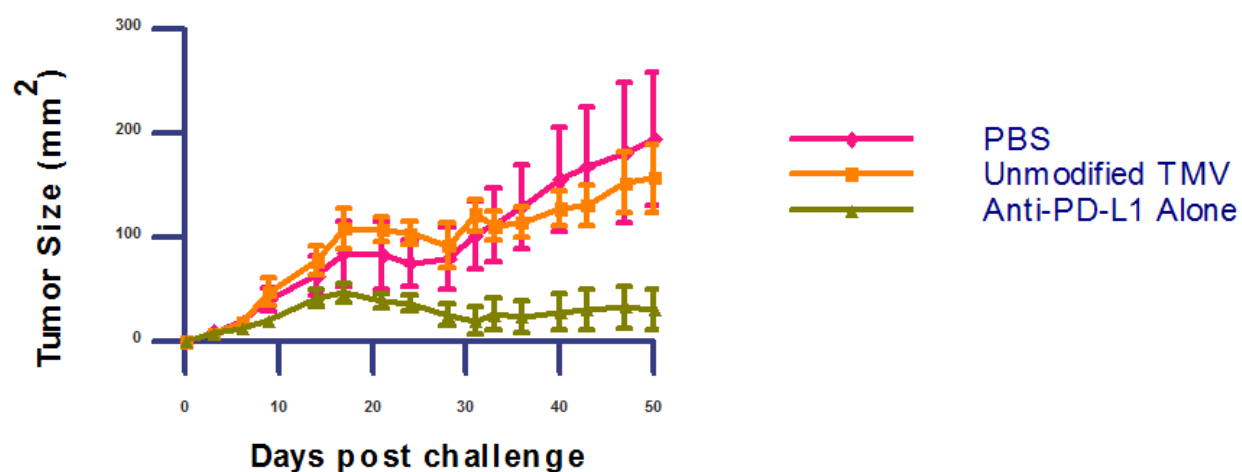


Figure 11: Anti-PD-L1 monotherapy of mice (for each group, n=5.) reduces E0771 tumor size, shown by comparison of average 4T07 tumor size of mice treated with PBS, unmodified TMV, and anti-PD-L1 antibody alone. TMVs. The size difference became significant on day 36 and continued until the experimental endpoint.

When compared to PBS-treated and unmodified TMV-treated mice, combination therapy-receiving mice saw statistically significantly smaller tumor sizes when compared to PBS-treated mice ( $P < 0.01$ ) on days 47 and 50 (Figure 12).

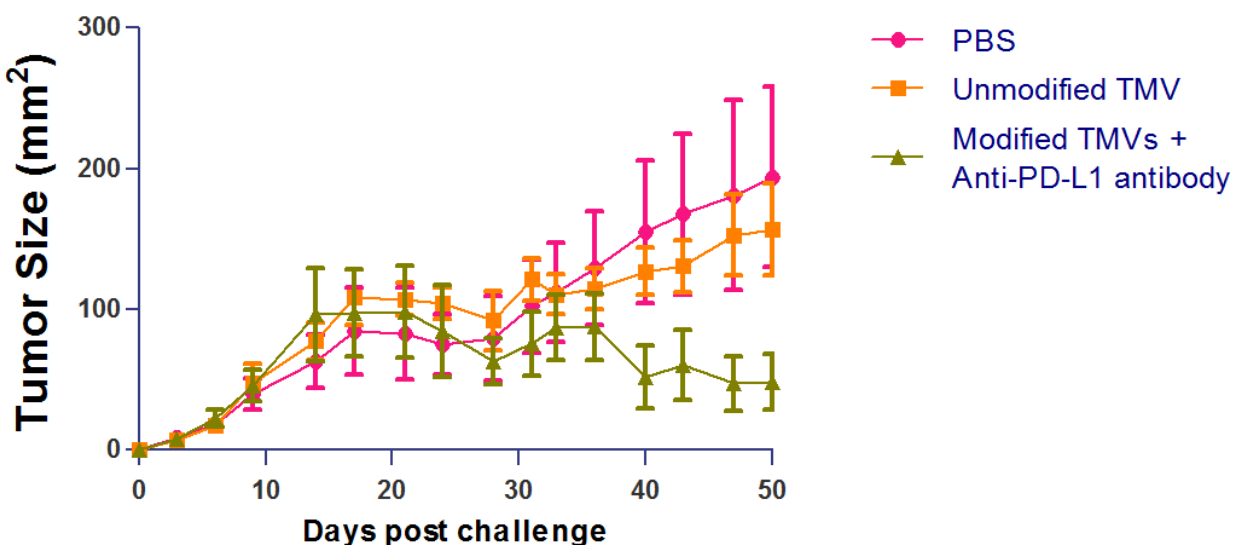


Figure 12: Combination therapy of mice (for each group, n=5.) consisting of GPI-mIL-12 + GPI-mB7-1 modified TMVs and anti-PD-L1 antibody reduces tumor size, as shown by comparison of average 4TO7 tumor size of mice treated with PBS, unmodified TMV, and modified TMV with anti-PD-L1 antibody combination therapy. The size difference became significant at day 47.

Both monotherapies were compared with the combination therapy by tracking average tumor size of treated mice (Figure 13). When comparing both monotherapies to each other, there was no statistically significant difference in average tumor size ( $P > 0.05$ ). Furthermore, there was no statistically significant difference in average tumor size between either monotherapy and the combination therapy ( $P > 0.05$ ).

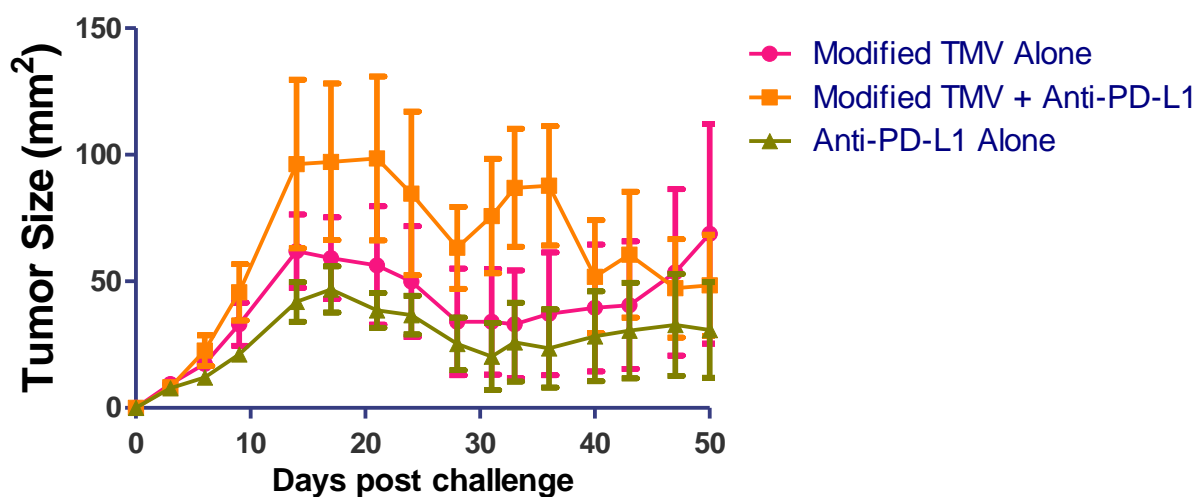


Figure 13: Treatment of mice (for each group, n=5.) with GPI-mIL-12 + GPI-mB7-1 modified TMVs, anti-PD-L1 antibody, or combination therapy of both yields statistically similar tumor sizes, as shown by comparison of average 4TO7 tumor size of mice treated with only TMVs modified with GPI-mIL-12 and GPI-mB7-1, only anti-PD-L1 antibody, or both. There was no statistically significant difference between tumor sizes across all three groups ( $P > 0.05$ ).

#### Homogenization of E0771 tumor tissue yields TMVs

E0771 tumor tissue previously harvested and stored at  $-80^{\circ}\text{C}$  was used to generate TMVs. After

homogenization and centrifugation over a 41% sucrose solution, TMVs were harvested from

the interphase. Amount harvested was quantified via creation of a standard curve (Figure 14)

via a BCA protein approximation kit. 9 mg of TMVs were generated, at a concentration of 1.5

mg/ml.

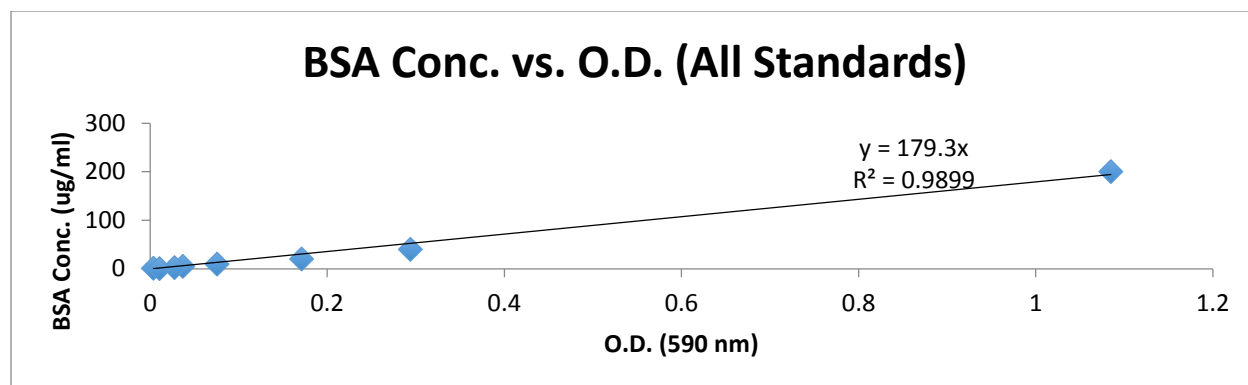


Figure 14: Standard curve generated via BCA protein approximation kit used to determine quantity and concentration of 4TO7-RG TMVs generated. 9 mg were generated from 2.84 g E0771 tumor tissue at a concentration of 1.5 mg/ml.

#### **Protein transfer of GPI-mB7-1 and GPI-mIL-12 onto E0771 TMVs**

GPI-mIL-12 and GPI-mB7-1 acquired from and tested for protein transfer competency by Dr. Chris Pack (MetEclipse Therapeutics) were incubated with E0771 TMVs for four hours at 37° C on an end-over-end rotator. Afterwards, unincorporated protein was washed away with PBS and centrifugation. To serve as a control, one group of TMVs was put through the same process sans GPI-proteins, called “mock protein transfer.” After protein transfer or mock protein transfer, TMVs were analyzed via flow cytometry to confirm successful protein transfer (Figure 15). Because of the rightward shift for both protein transfer of GPI-mIL-12 and GPI-mB7-1, we can see that the protein transfer was successful.

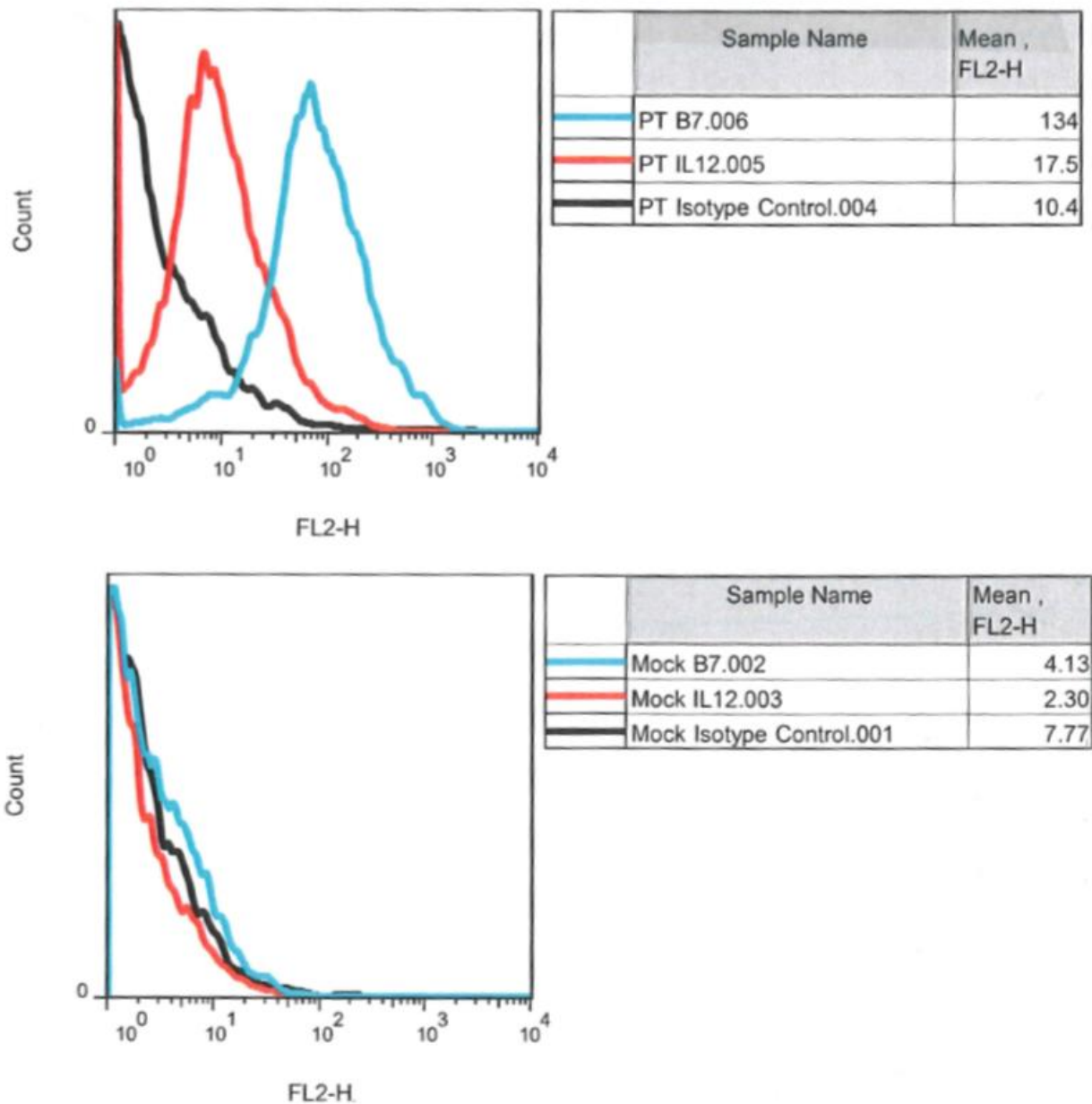


Figure 15: GPI-mIL-12 and GPI-mB7-1 incorporate onto E0771 TMVs. Comparison of TMVs protein transferred with GPI-mIL-12 and GPI-mB7-1 (top) and TMVs mock protein transferred with PBS in place of either GPI-ISM. The peak shift of the protein transferred TMVs shows that protein transfer of both proteins was successful.

**Prophylactic vaccination with any dose of protein-transferred (GPI-mIL-12 and GPI-mB7-1)**

**E0771 TMVs did not induce protection against E0771 live tumor cell challenge compared to**

**PBS vaccination**

Because we had never tried our vaccine with an E0771 tumor system, we wanted to determine what dose, if any, would have the greatest efficacy in reducing tumor burden. To this end, we used three different doses, administered according to the vaccination strategy outlined above. Despite our vaccine's success as a monotherapy in the 4T07 system, no dose (52.75  $\mu\text{g}$ , 105.5  $\mu\text{g}$ , or 211  $\mu\text{g}$ ) of TMVs modified with GPI-mIL-12 and GPI-mB7-1 yielded any significant difference ( $P > 0.05$ ) in tumor burden compared to treatment with PBS (control) or equal doses of unmodified E0771 TMV (Figure 16). Additionally, all mice were tumor free on day zero post-challenge, and all mice had measurable tumors by day 11 post-challenge.

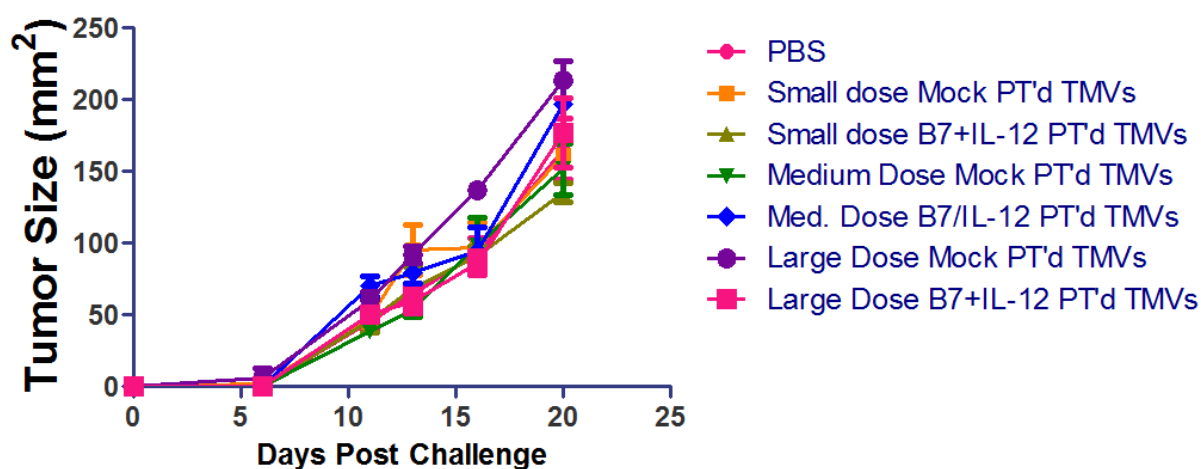


Figure 16: Comparison of average E0771 tumor size of mice treated with PBS (control) ( $n=7$ ), mock protein transferred E0771 TMVs ( $n=3$  per group), or E0771 TMVs modified with GPI-mIL-12 and GPI-mB7-1 ( $n=3$  per group). Error bars are SEM. There was no statistically significant difference between tumor sizes across all groups ( $P > 0.05$ ).

### E0771 tumor cells grown in culture express PD-L1

Because our GPI-mIL-12 + GPI-B7-1 modified TMV vaccine did not yield any statistically significant changes in tumor growth compared to controls, we wanted to examine why. We

hypothesized that this may be due to upregulation of immune checkpoint PD-L1, the ligand for PD-1 that, when bound to PD-1 on T cells, de-activates T cells. E0771 tumor cells were grown in culture and stained with anti-PD-L1 primary antibody to determine their PD-L1 expression level. As shown by experimental group's shift right compared to the unstained and isotype control groups, E0771 does express PD-L1 (Figure 17).

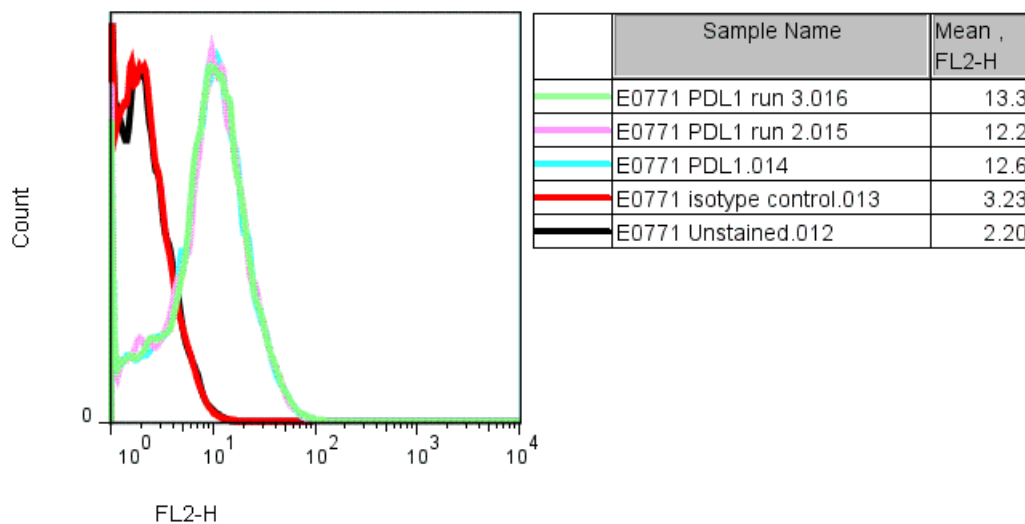


Figure 17: Cultured E0771 cells express PD-L1, as shown by the increase in MFI compared to unstained cells and cells stained with only the isotype control.

## **Discussion**

Here, we propose a tumor membrane vesicle-based therapy for breast cancer, utilizing GPI-anchor-driven protein transfer of immunostimulatory molecules IL-12 and B7-1. In the present study, we demonstrate that 4TO7RG TMVs modified by protein transfer to express the GPI-ISMs showed enhanced efficacy as a monotherapy against the 4TO7RG tumor cell challenge. We also studied the protein transfer-modified TMVs' efficacy as a combination therapy, used in conjunction with anti-CTLA-4 and anti-PD-L1 antibodies. Finally, we studied the efficacy of protein transfer-modified E0771 TMVs against the E0771 tumor cell line, another murine breast cancer cell line.

When used as a monotherapy to treat 4TO7 breast cancer, tumor burden was reduced in a statistically significant manner when compared to treatment with PBS (control) or unmodified TMVs. This suggests that tumor-specific immune responses were elicited by our GPI-ISM-modified TMV vaccine. We believe that vaccination with TMVs modified with GPI-mIL-12 and GPI-mB7-1 may yield protection due to humoral or cellular immune responses. The size of TMVs (data not yet published) is ideal for uptake by antigen presenting cells (APCs) such as dendritic cells (DCs) [42]. Because of this, we believe that dendritic cells may engulf the TMVs, then present out tumor antigens to T cells. This activates the T cells against the antigens being presented. Because cancers have been shown to produce inhibitors of DC maturation such as IL-10 [43], vascular endothelial growth factor (VEGF) [44], IL-6 [45], macrophage colony-stimulating factor (M-CSF) [45], and gangliosides [46], enhanced DC activation could be an important reason for our vaccine's efficacy.

One mechanism that may help this process involves B7-1 binding to CD28 on mast cells. This releases GM-CSF and TNF- $\alpha$ , both of which stimulate DCs, which then activate T cells. An alternate pathway involves IL-12 stimulating DCs, which then stimulate T cells. These pathways, combined with IL-12 and B7-1's ability to attract and prime T cells, respectively, may lead to a T cell response. Furthermore, IL-12 and B7-1 can also stimulate natural killer (NK) cells, which can then go on to also stimulate DCs, leading to a T cell response [47]. These potential pathways are summarized in Figure 18.

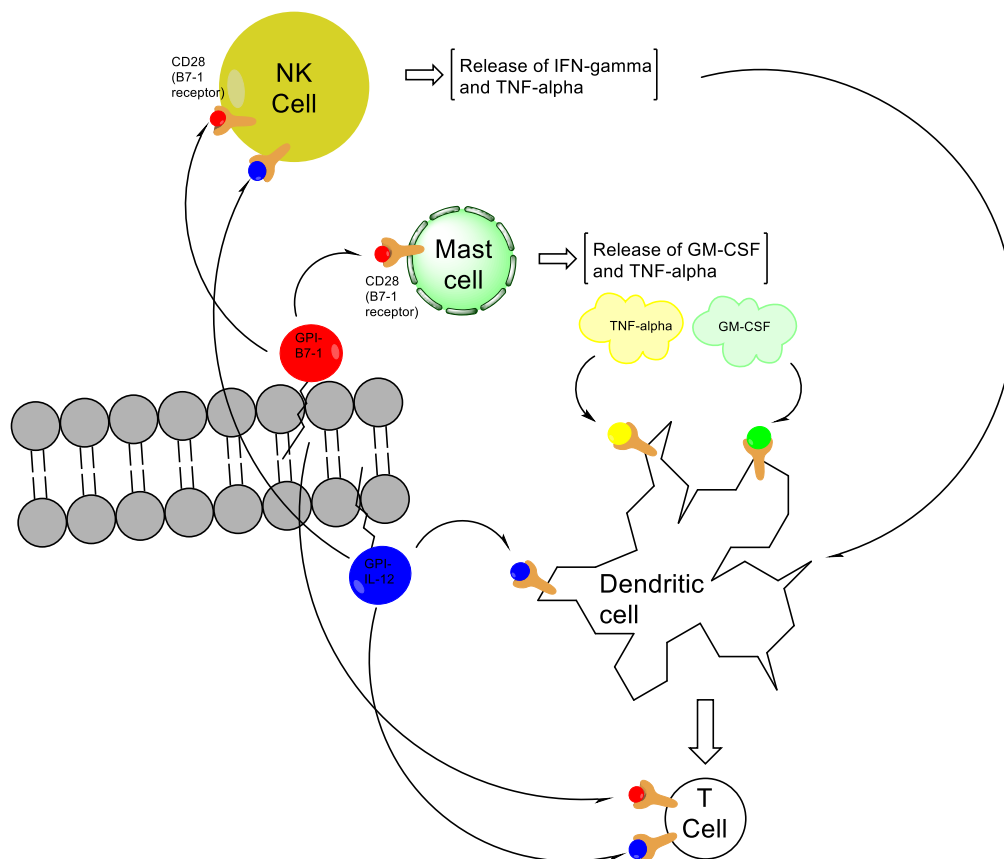


Figure 18: Simple schematic of potential pathways that may lead to direct or indirect (through DCs) T cell activation. Adapted from [47].

When used in combination with the anti-CTLA-4 antibody, average tumor size was statically the same when compared to monotherapy with either modified TMVs alone or anti-CTLA-4 antibody alone. Similarly, when used in combination with the anti-PD-L1 antibody, average tumor size was, again, statically the same when compared to monotherapy with either modified TMVs alone or the anti-PD-L1 antibody alone. However, these results do not rule out these combination therapies as potentially effective, especially in other cancer models. We believe that using a model that places a larger tumor burden on mice may allow for differences between the monotherapies and either combination therapy to become more clear, hopefully displaying greater efficacy.

Furthermore, it has been shown that efficacy of anti-PD-L1 antibody therapy can be predicted not only by amount of PD-L1 expressed on tumor cells, but also by PD-L1 being expressed by tumor-infiltrating immune cells [48]. The mechanism behind the correlation is still unclear [48]. We believe that this also may explain the lack of statistical difference between modified TMV monotherapy and modified TMV therapy augmented with anti-PD-L1 therapy. In order to test this, tumor-infiltrating cells need to be collected, and their level of PD-L1 expression must be determined.

When used as a monotherapy to treat E0771 breast cancer, none of our tested doses yielded any statistically significant change in average tumor size when compared to treatment with PBS (vehicle) or equal doses of unmodified E0771 TMVs. We believe that this may be due to upregulation of immune checkpoints such as PD-L1. We did note the presence of PD-L1 on cultured E0771 cells. However, more studies must be completed to determine if the amount of

PD-L1 expressed is enough to de-activate T cells. Furthermore, because PD-L1 expression may change in an *in vivo* setting, E0771 tumor tissue should be analyzed for PD-L1 expression.

T regulatory cells (Tregs) may also play a role in both the 4TO7 and E0771 settings. It has long been proposed that Tregs may promote tolerance to tumor cells [49-52]. Because Tregs have been shown to express CD25, Treg depletion studies using antibodies against CD25 could be performed to determine if this tumor tolerance, even in the presence of our therapy, is mediated by Tregs. Because it has been shown that intra-tumoral Tregs are more immunosuppressive than circulating Tregs [53], analysis of Treg levels in the tumor microenvironment may also be performed. If these results suggest that Tregs may be responsible for the immune-tolerance of these tumors, combination therapy of our modified TMV vaccine with anti-CD25 antibody may be a viable combination therapy. Previous studies showing that anti-CD25 monotherapy has been shown to be effective at treating cancer in a monotherapy [54] and tumor cell-loaded DC combination therapy [55] further the idea that this could be a viable combination therapy.

Although our studies were performed only using breast cancer models, TMVs can be prepared from any other tumor tissue as well. Therefore, our method of vaccine development can be implemented for use with any cancer that forms a solid tumor. Future studies will include testing our modified TMV-based therapy on other types of solid tumor-forming cancers, determining anti-metastatic efficacy of our TMV-based therapy, determining anti-metastatic efficacy of our TMV-based therapy when used with local therapies, as well as mechanistic studies aimed at elucidating the mechanism of action of our vaccine. To determine anti-metastatic efficacy of our vaccine, a clonogenic assay should be performed. This assay entails

challenging mice with live tumor cells, allowing the tumor to grow, then sacrificing the mice and isolating lung tissue. The lung tissue is then digested by collagenase, and the digested tissue is grown in media selecting for the cancer cells. After cancer cells are selected for, the plate is stained and colonies are counted, providing a quantifiable measure of lung metastasis. This was attempted for the E0771 study, but, because there is no known selection for E0771 cells, the assay's results were un-readable (data not shown). If no clonogenic assay can be developed for E0771 cells, H&E staining to analyze nodules in the lungs should be performed.

In order to mimic a patient's clinical experience, studies using our vaccine in combination with surgical removal of tumors should also be performed. Surgery can be a good first step because it will reduce the immediate local tumor burden, allowing for the memory immune response induced by our vaccine to serve as a continual systemic treatment, hopefully eliminating any tumor cells that metastasized prior to surgery or remain post-surgery, then metastasize. These studies are currently ongoing.

Studies analyzing our vaccine's mechanism of action should also be performed. For example, dependency on CD8+ or CD4+ T cells could be determined via cell depletion studies. If there appears to be a dependency on helper T cells, type of helper T cell involved could be determined by analyzing serum for increases in levels of IgG1 (associated with Th2 responses) or IgG2a and IgG2b (associated with Th1 responses) [56].

Overall, here, we show the efficacy of a GPI-mIL-12 + GPI-mB7-1 modified TMV vaccine in a 4TO7 breast cancer system. Although our combination therapy approaches did not appear to

bolster efficacy, and efficacy was not seen in the E0771 system, further studies must be performed to determine why.

**Financial & competing interest disclosure**

Dr. Selvaraj is a co-founder & equity holder of Metaclipse Therapeutics Corporation - a startup company formed to develop therapeutic cancer vaccines for humans using the protein transfer technology described here for which he is a co-inventor.

## **Appendix A: Publications**

Patel JM, **Vartabedian VF**, Selvaraj P. Lipid-mediated Cell Surface Engineering. Micro- and Nano Engineering of the Cell Surface 2014; Chapter 6: Pages 121-141 (ISBN: 978-1-4557-3146-6). (Edited by Weian Zhao and Jeffrey M. Karp, Elsevier Publications). [↗](#)

Cell membranes provide not only a physical barrier between the extracellular and intracellular space, but they also contain many proteins, which serve as mediators of inside-out and outside-in signals essential for cell survival and functions. Therefore, these cell surfaces can be engineered to manipulate cellular functions. Lipid-mediated protein transfer allows for decoration of the cell surface by exogenous incorporation of proteins that are modified with hydrophobic tails into lipid bilayers. Protein transfer allows for controllable expression of functional protein on the periphery of cells in an easy, time-efficient manner, and can be performed in either a direct one-step incorporation method or an indirect two-step incorporation method. This technology has led to breakthroughs in designing tumor vaccines, targeted-drug delivery, enhancing function of killer immune cells, and engineering antigen-presenting cells.

Jaina Patel, Sara He, Nikhil Amaram, Satoshi Yamanaka, **Vincent F. Vartabedian**, Vijayaraghavan Radhakrishnan, Jae Min Song, Rangaiah Shashidharamurthy, Richard Compans, Sang-moo Kang, and Periasamy Selvaraj. GPI-GM-CSF protein transferred onto H5 influenza VLPs remains stably expressed and functionally active. J Immunol May 2013 190 (Meeting Abstract Supplement) 66.17 [↗](#)

Pathogenic H5N1, a lipid-enveloped influenza virus, is a pandemic threat. The use of virus-like particles (VLPs) as an alternative to current influenza vaccines is highly promising. VLPs are similar in structure to their live viral counterparts but do not contain viral genome that is required for replication; hence VLPs provide for a safe and immunogenic vaccine. Although the particulate nature of VLPs allows them to be highly immunogenic, the need for protection against heterotypic viruses still remains. Therefore, inclusion of immunostimulatory molecules (ISMs) onto the VLP surface can help to induce cross-protection against strains and provide for stronger immunity. We were able to show that GPI-anchored-GM-CSF can incorporate stably onto H5 influenza VLP surfaces after a simple and quick protein transfer method. This method allows for the incorporation of the GPI-anchor onto the surface of lipid-bilayered VLPs within a matter of hours and allows for the incorporation of multiple GPI-ISMs in a concentration-dependent manner. Furthermore, protein transferred VLPs were functional in leading to bone marrow derived cell proliferation compared to unmodified VLPs, and incorporated GM-CSF was as functional as equal concentrations of commercially available recombinant soluble GM-CSF. Therefore, VLPs expressing GPI-GM-CSF could lead to enhanced immunogenicity and antiviral immune responses compared to unmodified VLPs.

Jaina M Patel, Gordon A Dale, **Vincent F Vartabedian**, Paulami Dey & Periasamy Selvaraj. Evaluation of: Davila ML, Riviere I, Wang X et al. Efficacy and toxicity management of 19-28z CAR T cell therapy in B cell acute lymphoblastic leukemia. *Sci. Transl. Med.* 6(224), 224ra25 (2014). *Immunotherapy* June 2014, Vol. 6, No. 6, Pages 675-678 [□](#)

Evaluation of: Davila ML, Riviere I, Wang X et al. Efficacy and toxicity management of 19-28z CAR T cell therapy in B cell acute lymphoblastic leukemia. *Sci. Transl. Med.* 6(224), 224ra25 (2014). Recently, chimeric antigen receptor (CAR) T-cell immunotherapy has entered clinical trials in patients with relapsed or refractory B-cell acute lymphoblastic leukemia. 19-28z CAR T cells express a fusion protein comprised of an anti-CD19 mAb fused with CD28 costimulatory and CD3-zeta-chain signaling domains. The current paper demonstrates that administration of 19-28z CAR T cells in patients with relapsed or refractory B-ALL in a Phase I clinical trial has led to 88% of patients undergoing complete remission. Despite the benefits, CAR T-cell therapy is associated with cytokine release syndrome toxicities. The authors demonstrated criteria to diagnose severe cytokine release syndrome (sCRS) and treated sCRS with either high-dose steroids or with tocilizumab, an IL-6 receptor-specific mAb. Although both alleviated sCRS, steroid treatment negated the beneficial effects of CAR T-cell therapy, whereas tocilizumab did not. Taken together, CAR T-cell immunotherapy can be used as a safe and effective approach against tumors with known tumor-associated antigens.

Patel, J. M., M. C. Kim, **V. F. Vartabedian**, Y. N. Lee, S. He, J. M. Song, H. J. Choi, S. Yamanaka, N. Amaram, A. Lukacher, C. Montemagno, R. W. Compans, S. M. Kang and P. Selvaraj. "Protein Transfer-Mediated Surface Engineering to Adjuvantate Virus-Like Nanoparticles for Enhanced Anti-Viral Immune Responses." *Nanomedicine*, (2015).

Recombinant virus-like nanoparticles (VLPs) are a promising nanoparticle platform to develop safe vaccines for many viruses. Herein, we describe a novel and rapid protein transfer process to enhance the potency of enveloped VLPs by decorating influenza VLPs with exogenously added glycosylphosphatidylinositol-anchored immunostimulatory molecules (GPI-ISMs). With protein transfer, the level of GPI-ISM incorporation onto VLPs is controllable by varying incubation time and concentration of GPI-ISMs added. ISM incorporation was dependent upon the presence of a GPI-anchor and incorporated proteins were stable and functional for at least 4 weeks when stored at 4°C. Vaccinating mice with GPI-granulocyte macrophage colony-stimulating factor (GM-CSF)-incorporated-VLPs induced stronger antibody responses and better protection against a heterologous influenza virus challenge than unmodified VLPs. Thus, VLPs can be enriched with ISMs by protein transfer to increase the potency and breadth of the immune response, which has implications in developing effective nanoparticle-based vaccines against a broad spectrum of enveloped viruses.

Jaina M. Patel, **Vincent F. Vartabedian**, Min-Chul Kim, Sara He, Sang-Moo Kang and Periasamy Selvaraj. Influenza virus-like particles engineered by protein transfer with tumor-associated antigens induces protective antitumor immunity. *Biotechno Bioeng*, (2015).

Delivery of antigen in particulate form using either synthetic or natural particles induces stronger immunity than soluble forms of the antigen. Among naturally occurring particles, virus-like particles (VLPs) have been genetically engineered to express tumor-associated antigens (TAAs) and have shown to induce strong TAA-specific immune responses due to their nano-particulate size and ability to bind and activate antigen-presenting cells. In this report, we demonstrate that influenza VLPs can be modified by a protein transfer technology to express TAAs for induction of effective antitumor immune responses. We converted the breast cancer HER-2 antigen to a glycosylphosphatidylinositol (GPI)-anchored form and incorporated GPI-HER-2 onto VLPs by a rapid protein transfer process. Expression levels on VLPs depended on the GPI-HER-2 concentration added during protein transfer. Vaccination of mice with protein transferred GPI-HER-2-VLPs induced a strong Th1 and Th2-type anti-HER-2 antibody response and protected mice against a HER-2-expressing tumor challenge. Soluble form of GPI-HER-2 induced only a weak Th2 response under similar conditions. These results suggest that influenza VLPs can be enriched with TAAs by protein transfer to develop effective VLP-based subunit vaccines against cancer without chemical or genetic modifications and thus preserve the immune stimulating properties of VLPs for easier production of antigen-specific therapeutic cancer vaccines.

## References

1. Siegel, R., et al., *Cancer statistics, 2014*. CA Cancer J Clin, 2014. **64**(1): p. 9-29.
2. DeSantis, C., et al., *Breast cancer statistics, 2013*. CA Cancer J Clin, 2014. **64**(1): p. 52-62.
3. Berry, D.A., et al., *Effect of screening and adjuvant therapy on mortality from breast cancer*. N Engl J Med, 2005. **353**(17): p. 1784-92.
4. Fisher, B., et al., *Twenty-year follow-up of a randomized trial comparing total mastectomy, lumpectomy, and lumpectomy plus irradiation for the treatment of invasive breast cancer*. N Engl J Med, 2002. **347**(16): p. 1233-41.
5. Greco, M., et al., *Breast cancer patients treated without axillary surgery: clinical implications and biologic analysis*. Ann Surg, 2000. **232**(1): p. 1-7.
6. McGuire, W.P., et al., *Cyclophosphamide and cisplatin compared with paclitaxel and cisplatin in patients with stage III and stage IV ovarian cancer*. N Engl J Med, 1996. **334**(1): p. 1-6.
7. Sledge, G.W., et al., *Phase III trial of doxorubicin, paclitaxel, and the combination of doxorubicin and paclitaxel as front-line chemotherapy for metastatic breast cancer: an intergroup trial (E1193)*. J Clin Oncol, 2003. **21**(4): p. 588-92.
8. Kessler, D.A., R.H. Austin, and H. Levine, *Resistance to chemotherapy: patient variability and cellular heterogeneity*. Cancer Res, 2014. **74**(17): p. 4663-70.
9. Sipos, F., M. Constantinovits, and G. Muzes, *Intratatumoral functional heterogeneity and chemotherapy*. World J Gastroenterol, 2014. **20**(10): p. 2429-32.
10. Li, X., et al., *Intrinsic resistance of tumorigenic breast cancer cells to chemotherapy*. J Natl Cancer Inst, 2008. **100**(9): p. 672-9.
11. Denisov, E.V., et al., *Intratatumoral morphological heterogeneity of breast cancer: neoadjuvant chemotherapy efficiency and multidrug resistance gene expression*. Sci Rep, 2014. **4**: p. 4709.
12. Jones, R.J., W.H. Matsui, and B.D. Smith, *Cancer stem cells: are we missing the target?* J Natl Cancer Inst, 2004. **96**(8): p. 583-5.
13. Petrella, T., et al., *Single-agent interleukin-2 in the treatment of metastatic melanoma: a systematic review*. Cancer Treat Rev, 2007. **33**(5): p. 484-96.
14. Mocellin, S., et al., *Interferon alpha adjuvant therapy in patients with high-risk melanoma: a systematic review and meta-analysis*. J Natl Cancer Inst, 2010. **102**(7): p. 493-501.
15. Hanahan, D. and R.A. Weinberg, *Hallmarks of cancer: the next generation*. Cell, 2011. **144**(5): p. 646-74.
16. Wolchok, J.D., et al., *Development of ipilimumab: a novel immunotherapeutic approach for the treatment of advanced melanoma*. Ann N Y Acad Sci, 2013. **1291**: p. 1-13.
17. Topalian, S.L., et al., *Survival, durable tumor remission, and long-term safety in patients with advanced melanoma receiving nivolumab*. J Clin Oncol, 2014. **32**(10): p. 1020-30.
18. Wolchok, J.D., et al., *Nivolumab plus ipilimumab in advanced melanoma*. N Engl J Med, 2013. **369**(2): p. 122-33.

19. Brahmer, J.R., et al., *Safety and activity of anti-PD-L1 antibody in patients with advanced cancer*. N Engl J Med, 2012. **366**(26): p. 2455-65.
20. Kantoff, P.W., et al., *Sipuleucel-T immunotherapy for castration-resistant prostate cancer*. N Engl J Med, 2010. **363**(5): p. 411-22.
21. Davila, M.L., et al., *Efficacy and toxicity management of 19-28z CAR T cell therapy in B cell acute lymphoblastic leukemia*. Sci Transl Med, 2014. **6**(224): p. 224ra25.
22. Patel, J.M., et al., *Cancer CARtography: charting out a new approach to cancer immunotherapy*. Immunotherapy, 2014. **6**(6): p. 675-8.
23. Niethammer, A.G., et al., *A DNA vaccine against VEGF receptor 2 prevents effective angiogenesis and inhibits tumor growth*. Nat Med, 2002. **8**(12): p. 1369-75.
24. Tamura, Y., et al., *Immunotherapy of tumors with autologous tumor-derived heat shock protein preparations*. Science, 1997. **278**(5335): p. 117-20.
25. Parkman, R., *Tumor hybrid cells: an immunotherapeutic agent*. J Natl Cancer Inst, 1974. **52**(5): p. 1541-5.
26. Low, M.G., *Glycosyl-phosphatidylinositol: a versatile anchor for cell surface proteins*. FASEB J, 1989. **3**(5): p. 1600-8.
27. McHugh, R.S., et al., *Construction, purification, and functional incorporation on tumor cells of glycolipid-anchored human B7-1 (CD80)*. Proc Natl Acad Sci U S A, 1995. **92**(17): p. 8059-63.
28. Nagarajan, S. and P. Selvaraj, *Glycolipid-anchored IL-12 expressed on tumor cell surface induces antitumor immune response*. Cancer Res, 2002. **62**(10): p. 2869-74.
29. McHugh, R.S., et al., *Protein transfer of glycosyl-phosphatidylinositol-B7-1 into tumor cell membranes: a novel approach to tumor immunotherapy*. Cancer Res, 1999. **59**(10): p. 2433-7.
30. Bozeman, E.N., et al., *Expression of membrane anchored cytokines and B7-1 alters tumor microenvironment and induces protective antitumor immunity in a murine breast cancer model*. Vaccine, 2013. **31**(20): p. 2449-56.
31. Coughlin, C.M., et al., *B7-1 and interleukin 12 synergistically induce effective antitumor immunity*. Cancer Res, 1995. **55**(21): p. 4980-7.
32. Ino, Y., et al., *Triple combination of oncolytic herpes simplex virus-1 vectors armed with interleukin-12, interleukin-18, or soluble B7-1 results in enhanced antitumor efficacy*. Clin Cancer Res, 2006. **12**(2): p. 643-52.
33. Putzer, B.M., et al., *Interleukin 12 and B7-1 costimulatory molecule expressed by an adenovirus vector act synergistically to facilitate tumor regression*. Proc Natl Acad Sci U S A, 1997. **94**(20): p. 10889-94.
34. Wen, X.Y., et al., *Tricistronic viral vectors co-expressing interleukin-12 (IL-12) and CD80 (B7-1) for the immunotherapy of cancer: preclinical studies in myeloma*. Cancer Gene Ther, 2001. **8**(5): p. 361-70.
35. Liu, J., et al., *The mechanism of exogenous B7.1-enhanced IL-12-mediated complete regression of tumors by a single electroporation delivery*. Int J Cancer, 2006. **119**(9): p. 2113-8.
36. Triozzi, P.L., et al., *Phase I study of the intratumoral administration of recombinant canarypox viruses expressing B7.1 and interleukin 12 in patients with metastatic melanoma*. Clin Cancer Res, 2005. **11**(11): p. 4168-75.

37. Shashidharamurthy, R., et al., *Immunotherapeutic strategies for cancer treatment: a novel protein transfer approach for cancer vaccine development*. *Med Res Rev*, 2012. **32**(6): p. 1197-219.
38. Heppner, G.H., F.R. Miller, and P.M. Shekhar, *Nontransgenic models of breast cancer*. *Breast Cancer Res*, 2000. **2**(5): p. 331-4.
39. Ewens, A., E. Mihich, and M.J. Ehrke, *Distant metastasis from subcutaneously grown E0771 medullary breast adenocarcinoma*. *Anticancer Res*, 2005. **25**(6B): p. 3905-15.
40. Otter, G.M. and F.M. Sirotnak, *Effective combination therapy of metastatic murine solid tumors with edatrexate and the vinca alkaloids, vinblastine, navelbine and vindesine*. *Cancer Chemother Pharmacol*, 1994. **33**(4): p. 286-90.
41. Johansen, P., et al., *Antigen kinetics determines immune reactivity*. *Proc Natl Acad Sci U S A*, 2008. **105**(13): p. 5189-94.
42. Manolova, V., et al., *Nanoparticles target distinct dendritic cell populations according to their size*. *Eur J Immunol*, 2008. **38**(5): p. 1404-13.
43. Gerlini, G., et al., *Metastatic melanoma secreted IL-10 down-regulates CD1 molecules on dendritic cells in metastatic tumor lesions*. *Am J Pathol*, 2004. **165**(6): p. 1853-63.
44. Gabrilovich, D.I., et al., *Production of vascular endothelial growth factor by human tumors inhibits the functional maturation of dendritic cells*. *Nat Med*, 1996. **2**(10): p. 1096-103.
45. Menetrier-Caux, C., et al., *Inhibition of the differentiation of dendritic cells from CD34(+) progenitors by tumor cells: role of interleukin-6 and macrophage colony-stimulating factor*. *Blood*, 1998. **92**(12): p. 4778-91.
46. Shurin, G.V., et al., *Neuroblastoma-derived gangliosides inhibit dendritic cell generation and function*. *Cancer Res*, 2001. **61**(1): p. 363-9.
47. Cimino, A.M., et al., *Cancer vaccine development: protein transfer of membrane-anchored cytokines and immunostimulatory molecules*. *Immunol Res*, 2004. **29**(1-3): p. 231-40.
48. Herbst, R.S., et al., *Predictive correlates of response to the anti-PD-L1 antibody MPDL3280A in cancer patients*. *Nature*, 2014. **515**(7528): p. 563-7.
49. Fujimoto, S., M. Greene, and A.H. Sehon, *Immunosuppressor T cells in tumor bearing host*. *Immunol Commun*, 1975. **4**(3): p. 201-17.
50. Berendt, M.J. and R.J. North, *T-cell-mediated suppression of anti-tumor immunity. An explanation for progressive growth of an immunogenic tumor*. *J Exp Med*, 1980. **151**(1): p. 69-80.
51. Bursuker, I. and R.J. North, *Generation and decay of the immune response to a progressive fibrosarcoma. II. Failure to demonstrate postexcision immunity after the onset of T cell-mediated suppression of immunity*. *J Exp Med*, 1984. **159**(5): p. 1312-21.
52. North, R.J. and I. Bursuker, *Generation and decay of the immune response to a progressive fibrosarcoma. I. Ly-1+2- suppressor T cells down-regulate the generation of Ly-1-2+ effector T cells*. *J Exp Med*, 1984. **159**(5): p. 1295-311.
53. Jie, H.B., et al., *Intratatumoral regulatory T cells upregulate immunosuppressive molecules in head and neck cancer patients*. *Br J Cancer*, 2013. **109**(10): p. 2629-35.
54. Jones, E., et al., *Depletion of CD25+ regulatory cells results in suppression of melanoma growth and induction of autoreactivity in mice*. *Cancer Immun*, 2002. **2**: p. 1.

55. Prasad, S.J., et al., *Dendritic cells loaded with stressed tumor cells elicit long-lasting protective tumor immunity in mice depleted of CD4+CD25+ regulatory T cells*. J Immunol, 2005. **174**(1): p. 90-8.
56. Lefeber, D.J., et al., *Th1-directing adjuvants increase the immunogenicity of oligosaccharide-protein conjugate vaccines related to Streptococcus pneumoniae type 3*. Infect Immun, 2003. **71**(12): p. 6915-20.